Entropy stable Galerkin methods with suitable quadrature rules for hyperbolic systems with random inputs

Xinghui Zhong * Chi-Wang Shu †

March 11, 2022

Abstract

In this paper, we investigate hyperbolic systems with random inputs based on generalized polynomial chaos (gPC) approximations, which is one of the most popular methods for uncertainty quantification (UQ) and can be implemented with either the stochastic Galerkin (SG) method or the stochastic collocation (SC) method. One of the challenges for solving stochastic hyperbolic systems with the SG method is that the resulting deterministic system may not be hyperbolic. The lack of hyperbolicity may lead to the ill-posedness of the problem and the instability of numerical simulations. The main objective of this paper is to show that by approximating the solution in the random space with the SG method in a pseudo-spectral way with suitable quadrature rules, the SG scheme can be written as a SC scheme on a set of specific nodes. The resulting collocation scheme preserves the hyperbolicity of the original hyperbolic system, and is more efficient to implement. On the other hand, entropy conditions play an essential role in the well-posedness of hyperbolic conservation laws. Thus we approximate the resulted collocation scheme in space by the entropy stable nodal discontinuous Galerkin (DG) method [4], where the entropy stability is guaranteed by high order summation-by-parts operators, entropy conservative fluxes and entropy stable fluxes. Numerical experiments are performed to validate the accuracy and effectiveness of the proposed numerical schemes.

Keywords: Uncertainty quantification, hyperbolic systems, generalized polynomial chaos, entropy stable, DG methods, hyperbolicity-preserving

1 Introduction

In this paper, we investigate the impact of uncertainty on hyperbolic conservation laws, with our focus on the following one-dimensional system

$$\frac{\partial \mathbf{u}(x,t,\mathbf{z})}{\partial t} + \frac{\partial \mathbf{f}(\mathbf{u}(x,t,\mathbf{z}))}{\partial x} = 0, \tag{1.1}$$

where $\mathbf{u} = (u_1, \cdots, u_d)^T$ denotes the vector of state variables taking values in a convex set $\Omega \subset \mathbb{R}^d$, $\mathbf{f} = (f_1, \cdots, f_d)^T$ is the flux function, and $\mathbf{z} = (z_1, \cdots, z_{d_z}) \in \Omega_z \subset \mathbb{R}^{d_z}$, $d_z \geq 1$ are a set of mutually independent random variables characterizing the random inputs to the governing equation. The system (1.1) is assumed to be hyperbolic for each realization of $\mathbf{z}$, that is, the Jacobian matrix $\mathbf{f}'(\mathbf{u})$ is assumed to have d real eigenvalues and a complete set of eigenvectors for each $\mathbf{z} \in \Omega_z$.

*School of Mathematical Sciences, Zhejiang University, Hangzhou, 310027, China. zhongxh@zju.edu.cn

†Division of Applied Mathematics, Brown University, Providence, RI 02912, USA. chi-wang_shu@brown.edu

The uncertainty may arise from physical parameters, initial or boundary conditions, etc. Many numerical techniques have been developed to predict the behavior of physical systems with random inputs, among which the polynomial chaos (PC) methods have received intensive attention. The term "polynomial chaos" was coined by Nobert Wiener in [47], in which Hermite polynomials serve as an orthogonal basis for studying the decomposition of Gaussian stochastic processes. Inspired by Wiener's work, Ghanem and his collaborators started the original PC method using Hermite polynomials for many practical engineering problems (most with Gaussian uncertainties) with success, see [17] for an overview. Later, generalized polynomial chaos (gPC) was proposed in [54], where different kinds of orthogonal polynomials are chosen as a basis depending on the probability distribution of the random inputs and are adopted for improved representations of more general random processes. Being essentially a spectral approach in the random space, the gPC method exhibits fast rate of convergence when the solution depends smoothly on the random parameters, and is numerically easy to implement with either the stochastic collocation (SC) method or the stochastic Galerkin (SG) method. The SC method is based on the repetitive use of an established numerical code solving the deterministic model on a prescribed set of nodes in the random space, and thus is non-intrusive. Early works can be found in [45, 31, 53, 1, 50, 33, 44], etc. The SG method is based on a Galerkin projection of the model equations and usually results in a set of coupled deterministic equations. Hence the SG method needs new codes to deal with the larger, coupled systems of equations and is intrusive. We refer readers to the review paper [51] and the book [52] for more details of the gPC method.

Although the gPC method has been successfully applied to a large variety of problems, its application to uncertain hyperbolic problems is quite challenging. One of the difficulties is caused by the fact that for hyperbolic conservation laws, the resulting deterministic systems from the SG method are not always hyperbolic. For scalar conservation laws, the resulting SG systems are still hyperbolic [3, 22, 28]. For general hyperbolic systems, the authors in [46] proved that if the stochastic Jacobian matrix $\nabla_{\mathbf{u}}\mathbf{f}$ is symmetric or its eigenvectors are independent of the uncertainty, then the resulted SG system is hyperbolic. This theory provides another proof of the fact that the Galerkin system derived from an uncertain scalar conservation law is hyperbolic and can be applied to linear hyperbolic systems with uncertainty only on initial or boundary conditions. This theory was further verified for linear hyperbolic systems in [36]. The authors in [11] showed that the resulting SG systems for shallow water equations and Euler equations are not hyperbolic in some cases. Recently, a hyperbolicity study on the uncertain kinetic Fokker-Planck equation in [27] showed that, while the SG system at the kinetic level is hyperbolic, its fluid dynamic limit, the uncertain isentropic Euler equation, is not necessarily hyperbolic. The lack of hyperbolicity may lead to the ill-posedness of the initial or boundary problem and the instability of numerical simulations.

Many efforts were made to obtain the well-behaved and hyperbolicity-preserving SG system for hyperbolic conservation laws. In [35, 11], the authors reformulated the conservation laws in a symmetrically hyperbolic form in terms of the entropy variables, proved the resulting SG system is hyperbolic, and proposed an optimization-based method, called the intrusive polynomial moment method (IPMM) to compute the polynomial chaos expansion of entropy variables given the polynomial chaos expansion of the conserved variables. The optimization problem in IPMM needs to be solved for each cell and at each time step and is computationally expensive. Moreover, it is not easy to extend this method to a general hyperbolic system without a convex entropy pair. Another approach with Roe variable formulation was proposed for the Euler equation in [34] and for the shallow water equation in [16, 15]. Although effective, its extension to general systems is also very limited, due to the Roe linearization. A class of operator-splitting based SG methods was developed for Euler equations in [5] and for the Saint-Venant system in [6], where the original systems are split into several subsystems whose SG systems are hyperbolic. However, the authors in [37] showed that this may still lead to complex eigenvalues due to the mismatch in hyperbolicity sets of the subsystems. The authors in [48, 49] carried out

a special treatment with symmetrization for quasi-linear hyperbolic conservation laws so that the resulting SG system is provably symmetric hyperbolic. Unfortunately the resulting SG systems are non-conservative and numerical solvers designed for conservative formulations cannot be applied directly. Recently, the authors in [37, 38, 12] applied a suitable "slope" limiter to the standard SG polynomial expansion that point-wisely shifts the solution into the numerically hyperbolicity set. More recently, a hyperbolicity-preserving SG approach for shallow water equations was proposed in [9, 10] by carefully selecting the polynomial chaos expansion of the nonlinear term q^2/h (we use the notations in [9] with q being the water discharge and h being the water height) in terms of the polynomial chaos expansions of the conserved variables.

In this paper, we quantify the uncertainties of hyperbolic systems by the SG method in a pseudo-spectral way. We show that with suitable quadrature rules, the SG scheme under a pseudo-spectral approximation leads to a collocation type scheme, which preserves the hyperbolicity of the original hyperbolic system and can be computed in a non-intrusive way. The idea to show that the Galerkin method leads to a collocation type approximation with the help of quadrature rules was inspired by [13] for studying polynomial approximations of ordinary differential equations and elliptic equations. We refer readers to [1] for the analysis of the analogies between the collocation and the spectral Galerkin methods for elliptic equations with random inputs. On the other hand, it is well-known that weak solutions of the hyperbolic system (1.1) may not be unique or physically relevant, and the physically relevant solution, i.e. the so-called entropy solution, satisfies the following entropy inequality

$$\frac{\partial U(\mathbf{u})}{\partial t} + \frac{\partial F(\mathbf{u})}{\partial x} \leq 0, \tag{1.2}$$

in the sense of distribution for convex entropy functions $U(\mathbf{u})$ and the associated entropy fluxes $F(\mathbf{u})$, both being mappings from Ω to $\mathbb{R}$ and related by

$$U'(\mathbf{u})\mathbf{f}'(\mathbf{u}) = F'(\mathbf{u}). \tag{1.3}$$

It is natural to seek numerical solutions which also share a similar entropy inequality as (1.3). In this paper, for the spatial discretization of the resulted collocation scheme, we apply the entropy stable discontinuous Galerkin (DG) methods proposed in [4], in which a unified framework was developed for designing high order DG methods satisfying a discrete version of (1.3) for any given single convex entropy, through suitable numerical quadrature which is specific to this given entropy. More details on the development of entropy stable schemes for hyperbolic conservation laws can be find in [4] and the cited references therein. We refer readers to [18] for the study on existence and uniqueness of random entropy admissible solutions for conservation laws, as well as the performance of the numerical method involving the SC method for the stochastic discretization and the standard Runge-Kutta DG methods [8] for the spatial-temporal discretization.

The rest of the paper is organized as follows: In Section 2, we present the gPC method for the hyperbolic system with random inputs, and show that under suitable quadrature rules, the SG scheme approximated in a pseudo-spectral fashion results a collocation type scheme. In Section 3 we present the details of the entropy stable DG method for the resulted collocation scheme from Section 2. Numerical tests are given in Section 4 and concluding remarks are given in Section 5.

2 Modeling stochastic hyperbolic systems

In this section, we discuss the gPC method for quantifying the uncertainties in the hyperbolic system (1.1).

2.1 The stochastic Galerkin and stochastic collocation methods

In this section, we briefly review the stochastic Galerkin (SG) method and the stochastic collocation (SC) method for discretizing (1.1) in the random space.

For easy presentation, let us consider $d_z = 1$ and assume z is a random variable in a properly defined complete random space with sample space Ω_z and probability density function $\mu(z)$. The gPC basis functions, denoted as $\{\varphi_m(z)\}_{m=0}^N$, are orthogonal polynomials with $\mu(z)$ serving as the weight function, i.e.

$$\int_{\Omega_z} \varphi_i(z)\varphi_j(z)\mu(z)dz = \delta_{ij}, \tag{2.1}$$

where δ_{ij} is the Kronecker delta function. Note the polynomials are normalized here for simplicity and they depend on the distribution of the random variable $\mathbf{z}$. For example, uniform distributions are associated with Legendre polynomials, and Gaussian distributions are associated with Hermite polynomials. See e.g. [54, 52] for more details. Let $\mathbb{P}_N(\Omega_z)$ be the set of polynomials of degree up to N defined in Ω_z. Clearly $\{\varphi_m\}_{m=0}^N$ form a basis of $\mathbb{P}_N(\Omega_z)$. Given a function $u : \Omega_z \to \mathbb{R}$, we denote the expected value (if exists) by

$$\mathbb{E}[u] := \int_{\Omega_z} u(z)\,\mu(z)\,\mathrm{d}z, \tag{2.2}$$

and the gPC projection of u is given by

$$u_N(z) = \sum_{m=0}^{N} \hat{u}_m\varphi_m(z), \quad \hat{u}_m = \mathbb{E}[u(z)\varphi_m(z)]. \tag{2.3}$$

The expectation and the gPC projection are also employed for functions $\mathbf{u} : \Omega_z \to \mathbb{R}^d$ by components.

For the SG method, we seek, for any fixed (x, t), an approximation $\mathbf{u}_N \in \mathbb{P}_N(\Omega_z)$ to the solution via a finite term gPC expansion

$$\mathbf{u}_N(x, t, z) = \sum_{i=0}^{N} \hat{\mathbf{u}}_i(x, t)\varphi_i(z), \tag{2.4}$$

such that the residue of the system (1.1) is orthogonal to the space $\mathbb{P}_N(\Omega_z)$ by components, i.e.

$$\frac{\partial}{\partial t}\int_{\Omega_z} \mathbf{u}_N(x, t, z)\ \varphi_m(z)\ \mu(z)\ \mathrm{d}z + \frac{\partial}{\partial x}\int_{\Omega_z} \mathbf{f}(\mathbf{u}_N)\ \varphi_m(z)\ \mu(z)\ \mathrm{d}z = 0, \quad m = 0, \cdots, N. \tag{2.5}$$

The result is a larger coupled deterministic system for the gPC expansion coefficients, given by

$$\frac{\partial}{\partial t}\hat{\mathbf{u}}_m(x, t) + \frac{\partial}{\partial x}\int_{\Omega_z} \mathbf{f}(\mathbf{u}_N(x, t, z))\varphi_m(z)\,\mu(z)\,\mathrm{d}z, \quad m = 0, \cdots, N. \tag{2.6}$$

For the stochastic collocation method, we seek, for any fixed (x, t), an approximation $\mathbf{v}_N \in \mathbb{P}_N(\Omega_z)$ to the solution such that the residue (by components) of the system (1.1) vanishes at a set of prescribed nodes $\{z^{(m)}\}_{m=1}^{N_c}$ in the random space, i.e.

$$\frac{\partial}{\partial t}\mathbf{v}_N(x, t, z^{(m)}) + \frac{\partial}{\partial x}\mathbf{f}(\mathbf{v}_N(x, t, z^{(m)})) = 0, \quad m = 1, \cdots, N_c. \tag{2.7}$$

The SG method ensures that the residue of the stochastic governing equations is orthogonal to the polynomial space spanned by the basis and thus has optimal accuracy, while the SC method only needs to execute a reliable deterministic solver at each node and thus is easy to implement. More details about the SG and SC methods can be found in the book [52]. Our focus in this paper is not on the comparison between these two methods. Instead, we show in the following section that the SG method under pseudo-spectral approach is equivalent to the SC method with special choice of nodes. In fact, for the SG method, a feasible treatment for the computation of nonlinear fluxes in the hyperbolic system is to approximate the integral (2.6) in a pseudo-spectral way [29], for which one can employ a quadrature rule, or a cubature rule in multivariate cases, with sufficient accuracy.

2.2 Pseudo-spectral approach

In this section, our aim is to show that the SG scheme (2.5) computed in a pseudo-spectral way leads to a collocation type scheme, which preserves the hyperbolicity property of the original hyperbolic system.

Let $\zeta_m,\ 0 \le m \le N$ be the zeros of $\varphi_{N+1}(z)$ and $l_m(z),\ 0 \le m \le N$ be the set of Lagrange interpolation polynomials with respect to the $N+1$ points $\{\zeta_m\}$, i.e. $l_m(\zeta_\ell) = \delta_{m\ell}$. The following expression is easily proven

$$l_m(z) = \prod_{\ell=0,\ell\neq m}^{N} \frac{z-\zeta_\ell}{\zeta_m-\zeta_\ell}. \tag{2.8}$$

Clearly $l_m(z) \in \mathbb{P}_N(\Omega_z)$ and $\{l_m\}_{m=0}^N$ form a basis of $\mathbb{P}_N$. For any polynomial $\varphi \in \mathbb{P}_N(\Omega_z)$, it can be written as

$$\varphi(z) = \sum_{m=0}^{N} \varphi(\zeta_m) l_m(z). \tag{2.9}$$

We define the interpolation operator $I_N : C^0(\Omega_z) \to \mathbb{P}_N(\Omega_z)$ which maps a continuous function f to the unique polynomial $I_N f \in \mathbb{P}_N(\Omega_z)$ satisfying $I_N f(\zeta_m) = f(\zeta_m),\ 0 \le m \le N$. That is

$$I_N f(z) = \sum_{m=0}^{N} f(\zeta_m) l_m(z). \tag{2.10}$$

The integral of f can by approximated by the integrating $I_N f$, i.e.

$$\int_{\Omega_z} f(z)\mu(z)\mathrm{d}z \approx \sum_{m=0}^{N} f(\zeta_m)\alpha_m, \tag{2.11}$$

where $\alpha_m = \int_{\Omega_z} l_m(z)\mu(z), \mathrm{d}z,\ 0 \le m \le N$ are the weights. This Gauss quadrature rule (2.11) is exact for any polynomial of degree up to $2N+1$, see e..g. [21, 13, 25] for more details.

The Galerkin procedure (2.5) holds for $\varphi_m, m = 0, \cdots, N$, which form a basis of $\mathbb{P}_N(\Omega_z)$. Therefore, for any $\varphi(z) \in \mathbb{P}_N(\Omega_z)$, we have

$$\frac{\partial}{\partial t}\int_{\Omega_z} \mathbf{u}_N(x,t,z)\ \varphi(z)\ \mu(z)\ \mathrm{d}z + \frac{\partial}{\partial x}\int_{\Omega_z} \mathbf{f}(\mathbf{u}_N)\ \varphi(z)\ \mu(z)\ \mathrm{d}z = 0. \tag{2.12}$$

By approximating the integrals in (2.12) by the Gauss quadrature rule with nodes $\{\zeta_m\}_{m=0}^N$ and weights $\{\alpha_m\}_{m=0}^N$, we obtain

$$\sum_{\ell=0}^{N} \frac{\partial}{\partial t}\mathbf{u}_N(x,t,\zeta_\ell)\varphi(\zeta_\ell)\alpha_\ell + \sum_{\ell=0}^{N} \frac{\partial}{\partial x}\mathbf{f}(\mathbf{u}_N(x,t,\zeta_\ell))\varphi(\zeta_\ell)\,\alpha_\ell = 0. \tag{2.13}$$

Then we take the test function φ as the Lagrange interpolation polynomials l_m, $0 \le m \le N$, which is also a basis of $\mathbb{P}_N(\Omega_z)$, yielding

$$\frac{\partial}{\partial t}\mathbf{u}_N(x,t,\zeta_m) + \frac{\partial}{\partial x}\mathbf{f}(\mathbf{u}_N(x,t,\zeta_m)) = 0, \quad m = 0, \cdots, N. \tag{2.14}$$

Now we obtain a collocation type approximation on the quadrature points $\{\zeta_m\}$ by approximating the SG method with quadrature rules. The specific quadrature rule through which the SG method leads to the SC method first needs to take a suitable number of points, i.e. $N+1$ points for the N-term Galerkin expansion, for the Lagrangian interpolation polynomials based on $N+1$ points to form a basis of $\mathbb{P}_N(\Omega_z)$ and thus can be taken as test functions in the Galerkin procedure. Secondly, it is well-known that numerical integral formulas based on $N+1$ points can not be exact for polynomials of degree higher than $2N+1$. The Gauss quadrature rule (2.11) with $N+1$ points on the other hand is exact for polynomials of degree up to $2N+1$. Therefore, the collocation points need to be taken as Gauss quadrature points in order to approximate the integrals in the SG scheme (2.12) with optimal accuracy, where the integrand of the first integral is a polynomial of degree up to $2N$ and the integrand of the second integral is a nonlinear function. A small difference between the Galerkin scheme and the collocation scheme is due to the so-called aliasing error, but the approximation solutions behave similarly. The collocation approximation in (2.14) is more efficient in term of computational cost and it preserves the hyperbolicity of the deterministic system.

Though we use one-dimensional ($d_z = 1$) random variable for the discussion, the generalization to multi-dimensional random variables is straightforward by tensor product collocation, which is mostly used for low-dimensional problems with d_z typically less than 5. For higher dimensions, an alternative approach is to use Smolyak sparse grids [40]. The Smolyak algorithm is a linear combination of product formulas, and the linear combination is chosen in such a way that an integration property for one dimension is preserved for higher dimensions as much as possible. Only products with a relatively small number of points are used and the resulting nodal set has a significantly smaller number of nodes compared to the tensor product rule. Depending on the choice of Gauss quadrature in one dimension, there are a variety of sparse grid constructions, which offer different accuracy. Here we do not engage in depth discussion of the technical details. We refer readers to [33] for error estimates of the SC method with the Smolyak-type sparse grids constructed based on Clenshaw-Curtis and Gaussian abscissas for solving stochastic partial differential equations. We also refer readers to [14, 55, 23] and cited references therein for the sparse grid SC method based on least square polynomial chaos.

3 Entropy stable discontinuous Galerkin methods

In this section, we present the algorithm formulation of the entropy stable nodal DG method [4] to approximate the resulted collocation scheme (2.14) for each fixed quadrature point ζ_m. For simplicity, we omit the argument ζ_m in this section.

3.1 Nodal DG scheme

In this section, we present a brief review of the nodal DG scheme. First we make a partition of the spatial domain $[a,b]$ into N_x computational cells and denote the cell by $I_i = [x_{i-1/2}, x_{i+1/2}]$, where

$$a = x_{\frac{1}{2}} < x_{\frac{3}{2}} < \cdots < x_{N_x+\frac{1}{2}}.$$

We denote the cell center by $x_i = \frac{1}{2}\left(x_{i-1/2} + x_{i+1/2}\right)$ and cell size by $\Delta x_i = x_{i+1/2} - x_{i+1/2}$, for $i = 1, \cdots, N_x$. Denote $\Delta x = \max\limits_{1\le i\le N_x} \Delta x_i$ and define a finite element approximation space as

$$\mathbb{V}_h^k := \{\mathbf{v}_h : \mathbf{v}_h|_{I_i} \in [\mathbb{P}_k(I_i)]^d, \;\; i = 1, \cdots, N_x\},$$

where $\mathbb{P}_k(I_i)$ denotes the set of polynomials of degree at most k on cell I_i.

With a slight abuse of notation, the semi-discrete classical DG scheme for solving (2.14) is defined as follows: for fixed t, to find the unique function $\mathbf{u}_h \in \mathbb{V}_h^k$, such that, for $i = 1, \cdots, N_x$,

$$\int_{I_i} \frac{\partial \mathbf{u}_h^T}{\partial t} \boldsymbol{\psi_h} \mathrm{d}x - \int_{I_i} \mathbf{f}(\mathbf{u}_h)^T \frac{\mathrm{d}\boldsymbol{\psi_h}}{\mathrm{d}x}\, \mathrm{d}x + \hat{\mathbf{f}}_{i+\frac{1}{2}}^T \boldsymbol{\psi_h}(x_{i+\frac{1}{2}}^-) - \hat{\mathbf{f}}_{i-\frac{1}{2}}^T \boldsymbol{\psi}_h(x_{i-\frac{1}{2}}^+) = 0, \tag{3.1}$$

holds for all test functions $\boldsymbol{\psi}_h \in \mathbb{V}_h^k$, where $\hat{\mathbf{f}}_{i+\frac{1}{2}}$ is the so-called numerical flux defined at the cell interface and depends on the values of $\mathbf{u}_h$ from both sides of the interface, i.e.

$$\hat{\mathbf{f}}_{i+\frac{1}{2}} = \hat{\mathbf{f}}(\mathbf{u}_h(x_{i+\frac{1}{2}}^-), \mathbf{u}_h(x_{i+\frac{1}{2}}^+)). \tag{3.2}$$

For systems, the numerical flux $\hat{\mathbf{f}}_{i+\frac{1}{2}}$ is taken as an exact or approximated Riemann solver. More details can be found in [7] and the review paper [8].

We now choose the local basis of the solution space $\mathbb{V}_k^h$ to be the Lagrangian polynomials based on the Legendre-Gauss-Lobatto points in the cell I_j, and obtain the nodal forms of the DG schemes. We first introduce some notations. Define the independent variable ξ in the reference cell $I = [-1, 1]$ via the following mapping

$$\xi = \frac{2(x - x_i)}{\Delta x}, \quad x \in [x_{i-\frac{1}{2}}, x_{i+\frac{1}{2}}]. \tag{3.3}$$

Denote $\xi_0, \xi_1, \cdots, \xi_k$ as the Legendre-Gauss-Lobatto quadrature points in $[-1, 1]$ and ω_i, $i = 0, \cdots, k$ as the associated quadrature weights. We further define the continuous inner product $(\cdot, \cdot)$ as $(\psi, \varphi) = \int_{-1}^1 \psi\varphi \mathrm{d}\xi$, and define the discrete inner product $\langle \cdot, \cdot \rangle$ as

$$\langle \psi, \varphi \rangle = \sum_{\ell=0}^{k} \psi(\xi_\ell)\varphi(\xi_\ell)\omega_\ell \tag{3.4}$$

by the Legendre-Gauss-Lobatto quadrature rule with $k + 1$ quadrature points, which is exact for polynomials of degree up to $2k - 1$. The Lagrangian basis polynomials based on $\{\xi_j\}_{j=0}^k$ are given by

$$L_j(\xi) = \prod_{\ell=0, \ell\neq j}^{k} \frac{\xi - \xi_\ell}{\xi_j - \xi_\ell}, \tag{3.5}$$

and the DG solution in the cell I_i can be represented by

$$\mathbf{u}_h(x, t) = \mathbf{u}_h(\xi, t) = \sum_{\ell=0}^{k} \tilde{\mathbf{u}}_i^\ell(t) L_\ell(\xi), \quad x \in I_i, \tag{3.6}$$

where $\tilde{\mathbf{u}}_i^\ell$ is a vector of length d containing the values of the solution $\mathbf{u}_h$ (a vector of length d) at the point ξ_ℓ in the cell I_i, i.e. $\tilde{\mathbf{u}}_i^\ell = \mathbf{u}_h|_{I_i}(\xi_l)$. After substituting (3.6) into (3.1) and applying Legendre-Gauss-Lobatto quadrature rule to the integrals in (3.1), the nodal formulation of the DG scheme is given by

$$\frac{\Delta x_i}{2} \sum_{l=0}^{k} M_{jl} \frac{\mathrm{d}\mathbf{u}^l}{\mathrm{d}t} - \sum_{l=0}^{k} S_{lj} \mathbf{f}^l + \sum_{l=0}^{k} B_{jl} \mathbf{f}_*^l = 0, \quad j = 0, \cdots, k, \tag{3.7}$$

where $\mathbf{u}^l = \tilde{\mathbf{u}}_i^l$, $\mathbf{f}^l = \mathbf{f}(\tilde{\mathbf{u}}_i^\ell)$, S is the stiffness matrix defined as $S_{jl} = \langle L_j, L_l' \rangle$, B is the boundary matrix given by $B = diag\{-1, 0, \cdots, 0, 1\}$, M is the mass matrix defined as $M_{jl} = \langle L_j, L_l \rangle = \omega_j \delta_{jl}$, and $\mathbf{f}_*^0 = \hat{\mathbf{f}}_{i-\frac{1}{2}}$, $\mathbf{f}_*^k = \hat{\mathbf{f}}_{i+\frac{1}{2}}, \mathbf{f}_*^l = 0, 1 \le l < k$. We remark here that the stiffness matrix S is integrated exactly since $L_j(\xi)L_l'(\xi)$ is a polynomial of degree $2k-1$, while the mass matrix M is obtained by the discrete inner product (3.4) which introduces some integration error and is typically termed as mass lumping.

3.2 Entropy stable nodal DG scheme

As discussed in [4], the nodal DG scheme (3.7) does not satisfy any entropy condition, but it can be modified to be entropy stable, due to the flexibility of the nodal representation. The key to this modification is the summation-by-parts (SBP) property, entropy conservative fluxes and entropy stable fluxes.

The SBP property is a discrete analogue of integration by parts, given by

$$S = MD, \quad MD + D^T M = S + S^T = B, \tag{3.8}$$

where D is the difference matrix with $D_{jl} = L_l'(\xi_j)$. By the SBP property (3.8), the nodal DG scheme (3.7) can be written as

$$\frac{\Delta x_i}{2} \frac{\mathrm{d}\mathbf{u}^j}{\mathrm{d}t} + \sum_{l=0}^{k} D_{jl}\mathbf{f}^l + \frac{\tau_j}{\omega_j}(\mathbf{f}_*^j - \mathbf{f}^j) = 0, \quad j = 0, \cdots, k, \tag{3.9}$$

where $\tau_0 = -1$, $\tau_k = 1$ and $\tau_j = 0$ for $1 \le j < k$.

To define the entropy conservative and stable fluxes, we first assume that the entropy function U is strictly convex, define the entropy variable as $\mathbf{v} = U'(\mathbf{u})^T$ and set $\mathbf{g}(\mathbf{v}) = \mathbf{f}(\mathbf{u}(\mathbf{v}))$. As claimed in [20, 32, 19], the existence of strictly convex entropy function is equivalent to the symmetry of $\mathbf{u}'(\mathbf{v})$ and $\mathbf{g}'(\mathbf{v})$, and thus there exist the so-called potential function $\phi(\mathbf{v})$ and potential flux $\psi(\mathbf{v})$ such that

$$\phi'(\mathbf{v}) = \mathbf{u}(\mathbf{v})^T, \quad \psi'(\mathbf{v}) = \mathbf{g}(\mathbf{v})^T. \tag{3.10}$$

A consistent, symmetric two-point numerical flux $\mathbf{f}_S(\mathbf{u}_L, \mathbf{u}_S)$ is entropy conservative if it satisfies

$$(\mathbf{v}_R - \mathbf{v}_L)^T \mathbf{f}_S(\mathbf{u}_L, \mathbf{u}_R) = \psi_R - \psi_L, \tag{3.11}$$

and a consistent two-point numerical flux $\hat{\mathbf{f}}(\mathbf{u}_L, \mathbf{u}_S)$ is entropy stable if it satisfies

$$(\mathbf{v}_R - \mathbf{v}_L)^T \hat{\mathbf{f}}(\mathbf{u}_L, \mathbf{u}_R) - (\psi_R - \psi_L) \le 0. \tag{3.12}$$

Here $\mathbf{v}_L, \mathbf{v}_R$ and ψ_L, ψ_R are the entropy variables and potential fluxes at the left and right states. More details can be found in [42, 43].

As shown in [4], the entropy stability of the nodal DG scheme is guaranteed by modifying (3.9) in the following form

$$\frac{\Delta x_i}{2} \frac{\mathrm{d}\mathbf{u}^j}{\mathrm{d}t} + \sum_{l=0}^{k} D_{jl}\mathbf{f}_S(\mathbf{u}^j, \mathbf{u}^l) + \frac{\tau_j}{\omega_j}(\mathbf{f}_*^j - \mathbf{f}^j) = 0, \quad j = 0, \cdots, k, \tag{3.13}$$

where $\mathbf{f}_S(\mathbf{u}^j, \mathbf{u}^l)$ is taken as the symmetric entropy conservative flux and the numerical flux $\hat{\mathbf{f}}$ is taken as the entropy stable flux at the cell interface. For the numerical flux $\hat{\mathbf{f}}$, it has been known for decades that the widely used upwind numerical fluxes, including monotone fluxes for scalar conservation laws and Godunov-type

fluxes for systems, are entropy stable. For the entropy conservative flux $\mathbf{f}_S(\mathbf{u}^j, \mathbf{u}^l)$, it is uniquely determined for scalar conservation laws but not unique for systems. For many systems, explicit entropy conservative fluxes can be derived and are easy to compute. Here we provide entropy conservative fluxes for general linear hyperbolic systems and Euler systems used in our numerical examples.

Example 3.1. The linear system is given by

$$\frac{\partial \mathbf{u}}{\partial t} + A\frac{\partial \mathbf{u}}{\partial x} = 0 \tag{3.14}$$

where A is a matrix independent of x and t and may depend on the random parameters. It is strictly hyperbolic for each realization of the random parameters.

- A is symmetric. As in [4], the entropy function can be taken as the standard energy $U = \frac{1}{2}\mathbf{u}^T\mathbf{u}$. Then $\mathbf{v} = \mathbf{u}$ and

$$F = \frac{1}{2}\mathbf{u}^T A\mathbf{u}, \quad \phi = \frac{1}{2}\mathbf{u}^T\mathbf{u}, \quad \psi = \frac{1}{2}\mathbf{u}^T A\mathbf{u}. \tag{3.15}$$

  The entropy stable flux is simply the arithmetic mean

$$\mathbf{f}_S(\mathbf{u}_L, \mathbf{u}_R) = \frac{1}{2}(A\mathbf{u}_L + A\mathbf{u}_R). \tag{3.16}$$

- A is not symmetric. We first need to get the symmetrizer of A and then transform the system into a symmetric one [24]. For better explanation, we use the wave equation (4.2) of Example 4.1 in Section 4, which is of the form (3.14) with

$$A = \begin{pmatrix} 0 & -1 \\ -c^2 & 0 \end{pmatrix}, \quad c > 0 \tag{3.17}$$

  as an example to show the procedure. The eigenvalues of A are $\pm c$ and the corresponding eigenvectors are $(1, \mp c)$. Let T be the matrix with columns being eigenvectors of A, then

$$T = \begin{pmatrix} 1 & 1 \\ c & -c \end{pmatrix}, \quad \text{and} \quad T^{-1} = \frac{1}{2}\begin{pmatrix} 1 & \frac{1}{c} \\ 1 & -\frac{1}{c} \end{pmatrix}. \tag{3.18}$$

  Let $\tilde{D} = \mathrm{diag}\{d_1, d_2\}$ be a real positive diagonal matrix. Then the so-called symmetrizer of A is defined as

$$H := (T^{-1})^* \tilde{D} T^{-1} = \frac{1}{4}\begin{pmatrix} d_1 + d_2 & \frac{1}{c}(d_1 - d_2) \\ \frac{1}{c}(d_1 - d_2) & \frac{1}{c^2}(d_1 + d_2) \end{pmatrix}, \tag{3.19}$$

  which is positive definite, and, with $d_1 = d_2 = 2$, we get the symmetrizer

$$H = (T^{-1})^* \tilde{D} T^{-1} = \begin{pmatrix} 1 & 0 \\ 0 & \frac{1}{c^2} \end{pmatrix}. \tag{3.20}$$

Let

$$H^{1/2} = \text{diag}\{1, 1/c\}, \quad \text{and} \quad \tilde{\mathbf{u}} = H^{1/2}\mathbf{u}, \tag{3.21}$$

then (3.14) can be transformed as

$$\frac{\partial \tilde{\mathbf{u}}}{\partial t} + H^{1/2}A(H^{1/2})^{-1}\frac{\partial \tilde{\mathbf{u}}}{\partial x} = 0, \tag{3.22}$$

with $\tilde{B} = H^{1/2}A(H^{1/2})^{-1} = \begin{pmatrix} 0 & -c \\ -c & 0 \end{pmatrix}$. The transformed system (3.22) is symmetric. As in the symmetric case, the entropy function can be taken as $U = \frac{1}{2}\tilde{\mathbf{u}}^T\tilde{\mathbf{u}}$. Then $\tilde{\mathbf{v}} = \tilde{\mathbf{u}}$ and

$$F = \frac{1}{2}\tilde{\mathbf{u}}^T\tilde{B}\tilde{\mathbf{u}}, \quad \phi = \frac{1}{2}\tilde{\mathbf{u}}^T\tilde{\mathbf{u}}, \quad \psi = \frac{1}{2}\tilde{\mathbf{u}}^T\tilde{B}\tilde{\mathbf{u}}. \tag{3.23}$$

The entropy conservative flux is

$$\mathbf{f}_S(\tilde{\mathbf{u}}_L, \tilde{\mathbf{u}}_R) = \frac{1}{2}(\tilde{B}\tilde{\mathbf{u}}_L + \tilde{B}\tilde{\mathbf{u}}_R). \tag{3.24}$$

By (3.21), the entropy function for the original system (3.14) with A defined in (3.17) can be taken as $U = \frac{1}{2}\tilde{\mathbf{u}}^T\tilde{\mathbf{u}} = \frac{1}{2}\mathbf{u}^T H\mathbf{u}$. Then $\mathbf{v} = H\mathbf{u}$ and

$$F = \frac{1}{2}\mathbf{u}^T HA\mathbf{u}, \quad \phi = \frac{1}{2}\mathbf{u}^T H\mathbf{u}, \quad \psi = \frac{1}{2}\mathbf{u}^T HA\mathbf{u}. \tag{3.25}$$

The entropy conservative flux is

$$\mathbf{f}_S(\mathbf{u}_L, \mathbf{u}_R) = \frac{1}{2}(A\mathbf{u}_L + A\mathbf{u}_R). \tag{3.26}$$

In fact, with $HA = H^{1/2}\tilde{B}H^{1/2}$ being Hermitian, we have

$$(\mathbf{v}_R - \mathbf{v}_L)^T\mathbf{f}_S(\mathbf{u}_L, \mathbf{u}_R) = \frac{1}{2}(\mathbf{u}_R - \mathbf{u}_L)^T HA(\mathbf{u}_R + \mathbf{u}_L) = \frac{1}{2}\mathbf{u}_R^T HA\mathbf{u}_R - \frac{1}{2}\mathbf{u}_L^T HA\mathbf{u}_L = \psi_R - \psi_L. \tag{3.27}$$

Example 3.2. The one-dimensional Euler system given by

$$\frac{\partial}{\partial t}\begin{pmatrix} \rho \\ \rho u \\ E \end{pmatrix} + \frac{\partial}{\partial x}\begin{pmatrix} \rho u \\ \rho u^2 + p \\ u(E+p) \end{pmatrix} = 0, \tag{3.28}$$

is of the form (1.1) with $\mathbf{u} = (\rho, \rho u, E)^T$ and $\mathbf{f}(\mathbf{u}) = \left(\rho u, \rho u^2 + p, u(E+p)\right)^T$. Here ρ is the density, u is the velocity, E is the total energy, and $p = (\gamma - 1)\left(E - \frac{1}{2}\rho u^2\right)$ is the pressure with γ being the ratio of specific heats. Denote

$$\Omega = \left\{\mathbf{u} = (\rho, \rho u, E)^T : \rho > 0,\ p > 0\right\} \tag{3.29}$$

as the physically admissible state set, where Ω is a convex set, and is related to the positivity of the density ρ and the pressure p. It can be verified that for all $\mathbf{u} \in \Omega$ and almost everywhere $\mathbf{z} \in \Omega_z$, the Euler system is hyperbolic.

For Euler systems, one entropy conservative flux suggested by Ismail and Roe in [26] is given by

$$\mathbf{f}_s(\mathbf{u}_L,\mathbf{u}_R)=\begin{pmatrix} f_S^{(1)}\\ f_S^{(2)}\\ f_S^{(3)}\end{pmatrix}=\begin{pmatrix} \overline{w_2}(\overline{w_3})^{\log}\\ \dfrac{\overline{w_3}}{\overline{w_1}}+\dfrac{\overline{w_2}}{\overline{w_1}}f_S^{(1)}\\ \dfrac{1}{2}\dfrac{\overline{w_2}}{\overline{w_1}}\left(\dfrac{\gamma+1}{\gamma-1}\dfrac{(\overline{w_3})^{\log}}{(\overline{w_1})^{\log}}+f_S^{(2)}\right)\end{pmatrix}, \tag{3.30}$$

where $(w_1,w_2,w_3)=\sqrt{\frac{\rho}{p}}(1,u,p)$, $\overline{w_\ell}$ and $(\overline{w_\ell})^{\log}$ are the arithmetic mean and the logarithmic mean given by

$$\overline{w_\ell}=\frac{1}{2}(w_{\ell,L}+w_{\ell,R}),\quad (\overline{w_\ell})^{\log}=\frac{w_{\ell,R}-w_{\ell,L}}{\log w_{\ell,R}-\log w_{\ell,L}},\quad \ell=1,2,3. \tag{3.31}$$

Another entropy conservative flux, suggested by Chandrashekar in [2] is given by

$$\mathbf{f}_s(\mathbf{u}_L,\mathbf{u}_R)=\begin{pmatrix} (\overline{u})^{\log}\overline{\rho}\\ \dfrac{\overline{\rho}}{\overline{\beta}}+\overline{u}f_S^{(1)}\\ \left(\dfrac{1}{(\gamma-1)(\overline{\beta})^{\log}}-\dfrac{1}{2}\overline{u^2}\right)f_S^{(1)}+\overline{u}f_S^{(2)}\end{pmatrix}, \tag{3.32}$$

where $\beta=\rho/p$.

In summary, we present in this section the details of the entropy stable DG scheme for approximating the spatial variable of the hyperbolic system on each quadrature point in the random space. For time discretization, we use the third-order strong stability preserving (SSP) Runge-Kutta (RK) method [39], which for solving

$$(u_h)_t=\mathcal{L}(u_h), \tag{3.33}$$

with $\mathcal{L}$ being the spatial discretization operator, is given by

$$\begin{aligned} u_h^{(1)}&=u_h^n+\Delta t\mathcal{L}(u_h^n),\\ u_h^{(2)}&=\frac{3}{4}u_h^n+\frac{1}{4}\left(u_h^{(1)}+\Delta t\mathcal{L}(u_h^{(1)})\right),\\ u_h^{n+1}&=\frac{1}{3}u_h^n+\frac{2}{3}\left(u_h^{(2)}+\Delta t\mathcal{L}(u_h^{(2)})\right).\end{aligned} \tag{3.34}$$

After obtaining the numerical solution $\mathbf{u}_h(x,t)$ at each quadrature point ζ_m in the random space, i.e. $\mathbf{u}_h(x,t,\zeta_m)$, the mean and variance of the numerical solution $\mathbf{u}_h$ at fixed spatial point x and time t are computed by

$$\mathbb{E}[\mathbf{u}_h](x,t)=\sum_{m=0}^{N}\mathbf{u}_h(x,t,\zeta_m)\alpha_m,\quad \mathrm{Var}[\mathbf{u}_h](x,t)=\sum_{m=0}^{N}\mathbf{u}_h(x,t,\zeta_m)^2\alpha_m-(\mathbb{E}[\mathbf{u}_h])^2, \tag{3.35}$$

according to the quadrature rule defined in (2.11). The corresponding standard deviation is $\sigma[\mathbf{u}_h]=\sqrt{\mathrm{Var}[\mathbf{u}_h]}$. Other statistical quantities of $\mathbf{u}_h$ can also be approximated by applying the the quadrature rule (2.11) directly to their definitions.

4 Numerical examples

In this section, we present numerical results to demonstrate the performance of the numerical scheme discussed in Sections 2 and 3. For all convergence tests, we examine the following two measures:

- error in the mean: $e_{mean}(t) = \max_x |\mathbb{E}(u) - \mathbb{E}(u_e)|$,
- error in the standard deviation (STD): $e_{std}(t) = \max_x |\sigma_u - \sigma_{u_e}|$,

where u and u_e denote the numerical solution and exact solution, respectively. For the accuracy tests of the entropy stable nodal DG methods coupled with the third-order SSP RK method, the time step Δt is further adjusted as $\Delta t \sim \Delta x^{4/3}$ for $k = 3$ and $\Delta t \sim \Delta x^{5/3}$ for $k = 4$.

Example 4.1. In this example, we test the convergence rates of the errors in the mean and in the STD for solutions with different regularity properties, using the following scalar wave equation

$$\frac{\partial^2 w}{\partial t^2} = c^2 \frac{\partial^2 w}{\partial x^2} \tag{4.1}$$

with velocity $c > 0$. Define $u_1 := \frac{\partial w}{\partial x}$ and $u_2 := \frac{\partial w}{\partial t}$. Equation (4.1) can be rewritten as the following system

$$\frac{\partial}{\partial t}\begin{pmatrix} u_1 \\ u_2 \end{pmatrix} + \begin{pmatrix} 0 & -1 \\ -c^2 & 0 \end{pmatrix} \frac{\partial}{\partial x}\begin{pmatrix} u_1 \\ u_2 \end{pmatrix} = \begin{pmatrix} 0 \\ 0 \end{pmatrix}. \tag{4.2}$$

We take $c(z) = 1 + 0.1z$ as random perturbations, where z is a uniformly distributed random variable on $[-1, 1]$. This linear system (4.2) is strictly hyperbolic for each realization of z. Let $\mathbf{u} = (u_1, u_2)^T$ and the system (4.2) can be written into the form (3.14) with A defined in (3.17). We consider the following two settings:

- **Case I:** Initial conditions are given by

$$u_{1,0}(x) = \sin x, \quad u_{2,0}(x) = 0, \tag{4.3}$$

  in the domain $x \in [0, 2\pi]$ and periodic boundary conditions are applied. $t = 2\pi$.

- **Case II**: Initial conditions are given by

$$u_{1,0}(x) = \begin{cases} 4x(x^2 - 1) & -1 < x < 1; \\ 0 & \text{elsewhere,} \end{cases} \quad \text{and} \quad u_{2,0}(x) = 0, \tag{4.4}$$

  in the domain $x \in [-5, 5]$ and the boundary conditions $\mathbf{u}(-5, t) = \mathbf{u}(5, t) = 0$ are applied [36]. $t = 3$.

For Case I, $u_{1,0}(x)$ is infinitely differentiable and thus belongs to the space $C^\infty([0, 2\pi], \mathbb{R})$. For Case II, $u_{1,0}(x)$ and its first derivative are L^2 functions, and thus it belongs to the Sobolev space $\mathbf{H}^1([-5, 5], \mathbb{R})$. The exact solution of (4.2) is

$$\begin{aligned} u_1(x, t, z) &= \frac{1}{2}\left(u_{1,0}(x + c(z)t) + u_{1,0}(x - c(z)t)\right), \\ u_2(x, t, z) &= \frac{c(z)}{2}\left(u_{1,0}(x + c(z)t) - u_{1,0}(x - c(z)t)\right). \end{aligned} \tag{4.5}$$

Therefore, the solution of (4.2) is sufficiently smooth under the settings of Case I, while the solution of (4.2) has finite regularity under the settings of Case II.

Numerical simulations are performed with the entropy function taken as $U = \frac{1}{2}\mathbf{u}^T H\mathbf{u}$, where the symmetrizer H is defined in (3.20), and the entropy stable flux is given by (3.26). The Lax-Friedrichs flux is adopted at cell interfaces. The basis of the gPC expansion is taken as the Legendre polynomials, and the quadrature points $\{\zeta_m\}_{m=1}^{N_z}$ are taken as the roots of the (N_z)-th Legendre polynomial, i.e. the Legendre-Gauss quadrature points. 20 Gauss-Legendre quadrature points are used to evaluate the mean and standard deviation of the exact solution.

We first show the convergence of the errors in the mean and the errors in the STD of the solution with different number of collocation points N_z for Case I in Figure 4.1 on the *semi-log* scale and for Case II in Figure 4.2 on the *log-log* scale, with $N_x = 320$ cells in the spatial domain. For Case I with sufficiently smooth solutions, we observe in Figure 4.1 the exponential convergence rate with respect to the number of collocation points N_z. The errors saturate when the spatial and temporal errors dominate. For Case II where the solutions have finite regularity, we observe in Figure 4.2 the second-order spectral convergence rate.

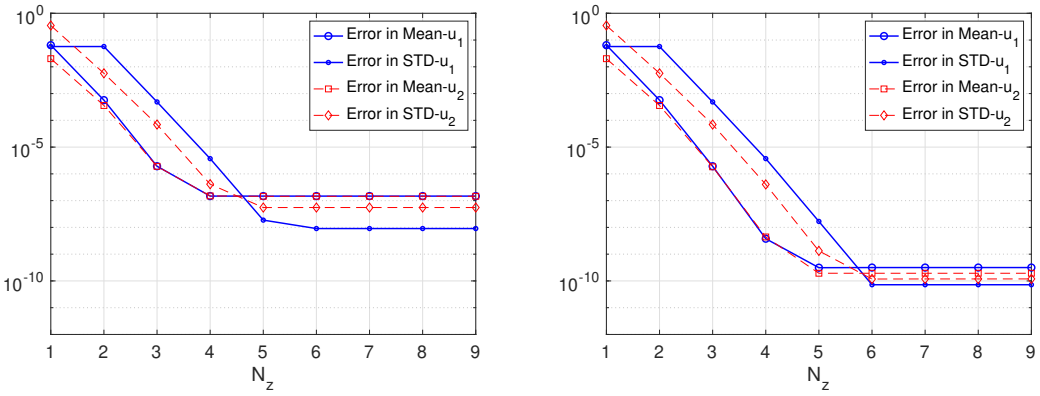

Figure 4.1: Wave equation (4.2). Case I. Errors in the mean and STD of the solution with respect to the number of collocation points N_z. DG scheme with $k = 2$ (left) and $k = 3$ (right). $N_x = 320$.

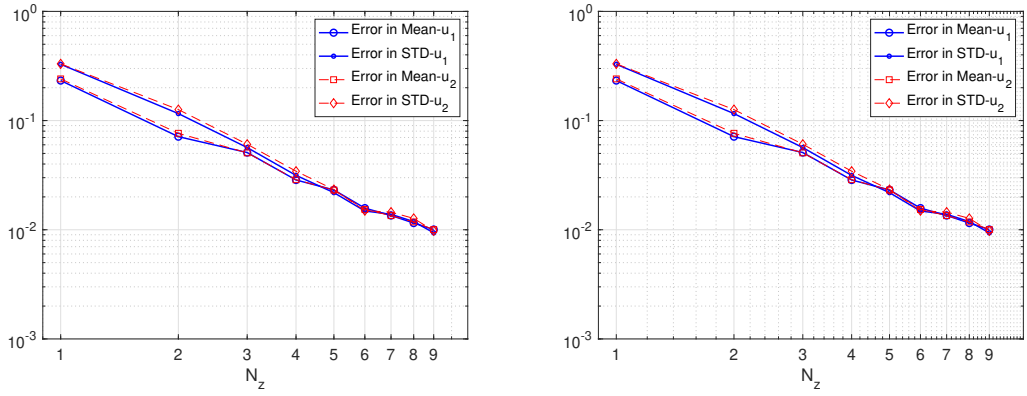

Figure 4.2: Wave equation (4.2). Case II. Errors in the mean and STD of the solution with respect to the number of collocation points N_z. DG scheme with $k = 2$ (left) and $k = 3$ (right). $N_x = 320$.

We then fix a relatively large $N_z = 8$ and conduct the convergence test of the errors in the mean and STD with respect to the entropy stable DG spatial discretization, for Case I with sufficiently smooth solutions. We

list numerical errors and orders of convergence with respect to different N_x in Table 4.1. We observe optimal convergence rate of $k+1$ for the DG scheme with $k+1$ nodes as expected.

Table 4.1: Wave equation 4.2. Case I. Errors and convergence rates in the mean and STD of the solution with respect to the DG spatial discretization. $N_z = 8$.

		u_1				u_2			
	N_x	e_{mean}	Order	e_{std}	Order	e_{mean}	Order	e_{std}	Order
$k=1$	20	2.37E-02		7.29E-03		9.13E-02	9	1.86E-02	
	40	2.72E-03	3.13	2.07E-03	1.81	2.44E-02	1.90	3.70E-03	2.33
	80	2.70E-04	3.33	5.33E-04	1.96	6.21E-03	1.98	7.86E-04	2.24
	160	1.97E-05	3.78	1.34E-04	1.99	1.56E-03	2.00	1.79E-04	2.14
$k=2$	20	5.86E-04		6.35E-05		4.93E-04		2.13E-04	
	40	7.50E-05	2.97	5.65E-06	3.49	6.81E-05	2.86	2.78E-05	2.94
	80	9.42E-06	2.99	6.12E-07	3.21	8.96E-06	2.93	3.51E-06	2.98
	160	1.18E-06	3.00	7.33E-08	3.06	1.15E-06	2.96	4.41E-07	2.99
$k=3$	16	4.96E-05		1.11E-05		3.03E-05		1.84E-05	
	32	3.14E-06	3.98	7.13E-07	3.96	1.92E-06	3.98	1.18E-06	3.97
	64	1.97E-07	3.99	4.49E-08	3.99	1.21E-07	3.99	7.39E-08	3.99
	128	1.23E-08	4.00	2.81E-09	4.00	7.54E-09	4.00	4.63E-09	4.00
$k=4$	16	7.87E-06		4.75E-07		7.69E-07		2.97E-06	
	32	2.44E-07	5.01	1.49E-08	5.00	2.86E-08	4.75	9.25E-08	5.00
	64	7.60E-09	5.00	4.65E-10	5.00	9.40E-10	4.93	2.89E-09	5.00
	128	2.37E-10	5.00	1.45E-11	5.00	3.00E-11	4.97	9.05E-11	5.00

For a more detailed visualization, we also perform the numerical simulation with fixed time step size in order to conveniently compute the time evolution of the statistical information of the numerical solution. We adopt the entropy stable DG scheme with $k = 2$ and $N_x = 100$ for the spatial discretization. We set $\Delta t = \frac{2\pi}{240}$ for Case I and $\Delta t = \frac{1}{80}$ for Case II. Clearly the CFL condition is satisfied, which is necessary for the stability of the method. We show the resulting solutions of the system (4.2) for the deterministic case with $c = 1$ in Figure 4.3 for Case I and in Figure 4.5 for Case II. Time evolutions of the mean and standard deviation of the solutions achieved by the collocation scheme with 4 points are shown in Figure 4.4 for Case I and in Figure 4.6 for Case II. The expected values of both cases are similar to the deterministic solution with $c = 1$.

Example 4.2. In this example, we solve the linearised shallow water equations. One-dimensional shallow water equations [30] are given by

$$\frac{\partial}{\partial t}\begin{pmatrix} v \\ h \end{pmatrix} + \frac{\partial}{\partial x}\begin{pmatrix} \frac{1}{2}v^2 + h \\ vh \end{pmatrix} = \begin{pmatrix} 0 \\ 0 \end{pmatrix} \tag{4.6}$$

with the water level $h > 0$ and the velocity $v \in \mathbb{R}$. The linearised shallow water equations are of the form

$$\frac{\partial}{\partial t}\mathbf{u} + A\frac{\partial}{\partial x}\mathbf{u} = \mathbf{0}. \tag{4.7}$$

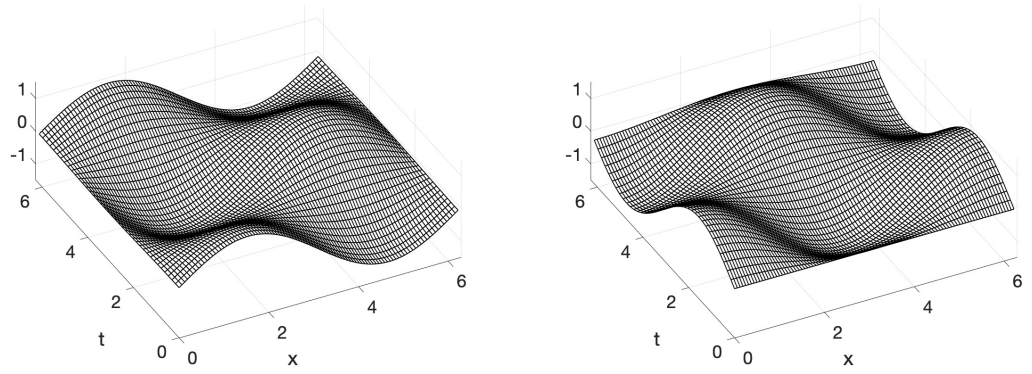

Figure 4.3: Numerical solutions u_1 (left) and u_2 (right) of wave equation (4.2) with $c = 1$. Case I. $k = 2$.

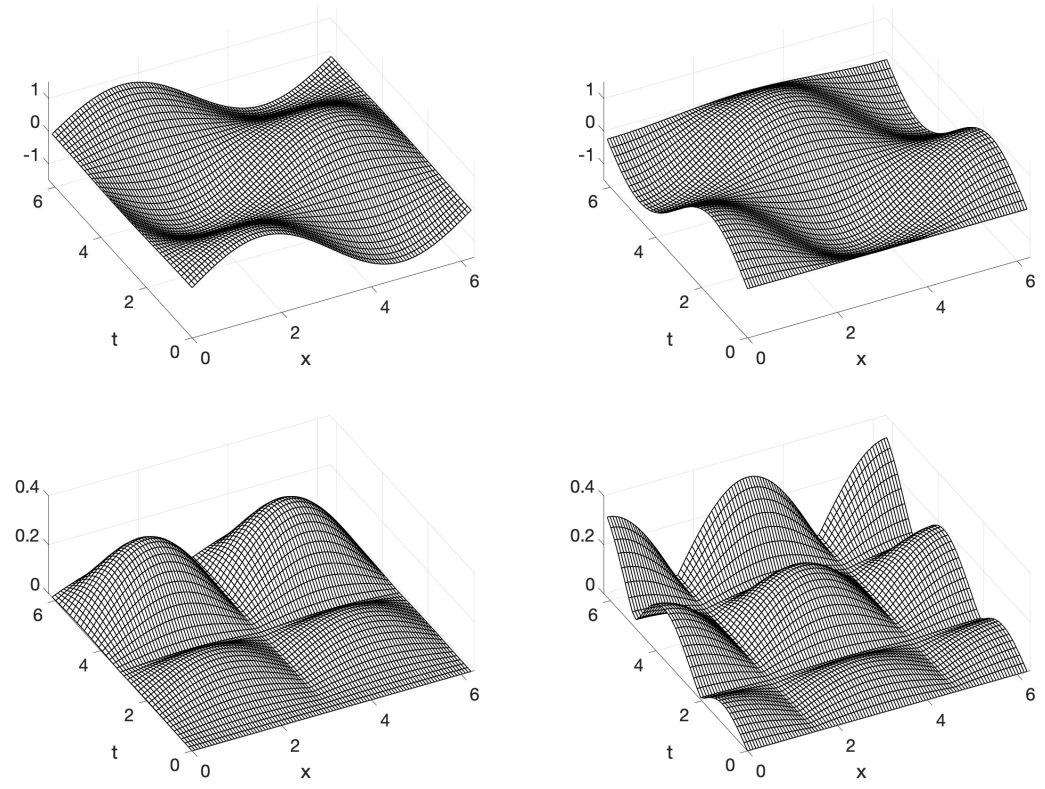

Figure 4.4: Mean (top) and standard deviation (bottom) of u_1 (left) and u_2 (right) of wave equation (4.2). Case I. $k = 2$. $N_z = 4$.

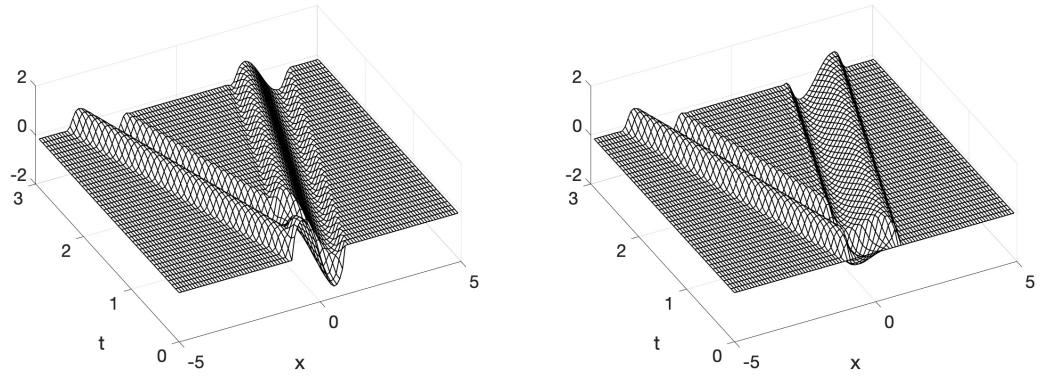

Figure 4.5: Numerical solutions u_1 (left) and u_2 (right) of wave equation (4.2) with $c = 1$. Case II. $k = 2$.

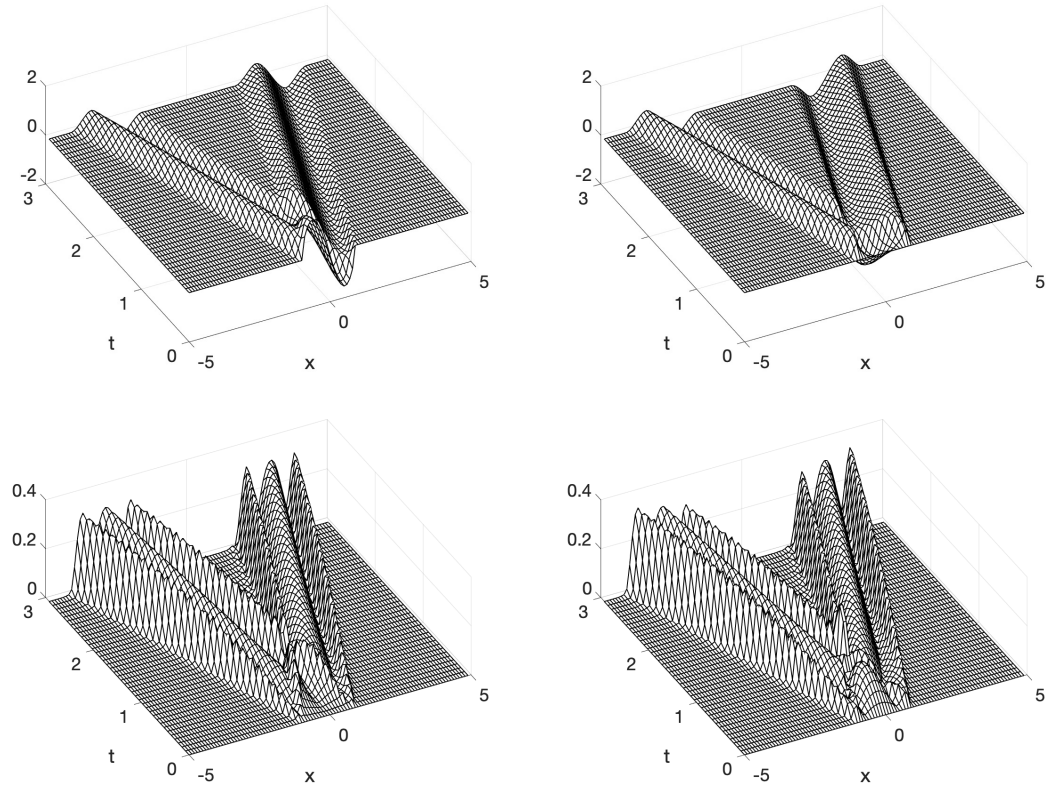

Figure 4.6: Mean (Top) and standard deviation (bottom) of u_1 (left) and u_2 (right) of wave equation (4.2). Case II. $k = 2$. $N_z = 4$.

where $\mathbf{u} = (u_1,\ u_2)^T$ and the coefficient matrix A is given by

$$A = \begin{pmatrix} \bar{v} & 1 \\ \bar{h} & \bar{v} \end{pmatrix}$$

with $\bar{v}$, $\bar{h}$ being constants. The linear system (4.7) is strictly hyperbolic for all $\bar{v} \in \mathbb{R}$ and all $\bar{h} > 0$. We take the constants $\bar{v} = 2$, $\bar{h} = \frac{1}{2}$ and add random perturbations, which yields the matrix A as

$$A(z_1, z_2) = \begin{pmatrix} 2 & 1 \\ \frac{1}{2} & 1 \end{pmatrix} + z_1\eta \begin{pmatrix} 2 & 0 \\ 0 & 2 \end{pmatrix} + z_2\eta \begin{pmatrix} 0 & 0 \\ \frac{2}{5} & 0 \end{pmatrix}. \tag{4.8}$$

Here the constant $\eta \in \mathbb{R}$ is used to control the magnitude of the variance in the random input. For the random variables, we consider the following two cases:

- **Case I:** Both z_1 are z_2 are uniformly distributed random variables on $[-1, 1]$;
- **Case II:** z_1 is a standard Gaussian random variable and z_2 is a uniformly distributed random variable on $[-1, 1]$.

For both settings, the linear system (4.7) is strictly hyperbolic for each realization of the random parameters provided that $|\eta| < \frac{5}{4}$. We set $\eta = 1$. We take the basis of the gPC expansion for two-dimensional random space by extending the one-dimensional basis via tensor construction. Thus the corresponding quadrature points in the random space are taken as the tensor product of two sets of Legendre-Gauss quadrature points for Case I, and the tensor product of Legendre-Gauss quadrature points and Hermite-Gauss quadrature points for Case II. We remark here that Case II serves as a counterexample in [36], in which the hyperbolicity of the resulted SG system is not guaranteed for a basis of multivariate polynomials up to a fixed degree.

We perform numerical simulations of the linearised system (4.7) under the same setting as in [36] with the initial conditions given by

$$u_1(0, x) = \frac{1}{10}\sin(2\pi x), \quad u_2(0, x) = \frac{1}{10}\cos(2\pi x),$$

and periodic boundary conditions applied for the spatial domain $[0, 1]$. The entropy function is taken as $U = \frac{1}{2}\mathbf{u}^T H\mathbf{u}$ with the symmetrizer H given by

$$H = \begin{pmatrix} 1 & 0 \\ 0 & \frac{10}{5+4z_2} \end{pmatrix}$$

and the entropy stable flux is given by (3.26). The Lax-Friedrichs flux is adopted at cell interfaces.

First, we conduct the convergence test for Case I. Figure 4.7 shows the convergence of the errors in the mean and standard deviation of the solution with respect to the number of quadrature points N_z ($N_z = 1, 4, 9, 25, \cdots$ for two-dimensional random space) on the semi-log scale, with $N_x = 160$ cells in the spatial domain for $k = 2,\ 3$. We observe the exponential convergence rate with respect to the number of collocation points for both DG schemes.

We also perform numerical tests for the DG scheme with $k = 2$ on $N_x = 25$ cells and fixed time step size. For comparison, we first solve the deterministic system (4.7) with $z_1 = z_2 = 0$, i.e., the mean of random parameters. Figure 4.8 shows the resulting deterministic solution with $\Delta t = \frac{1}{150}$. For both random cases, Δt is taken to be $\frac{1}{1600}$. Figures 4.9 and 4.10 show the mean and standard deviation of the numerical solution of Case I obtained by the SC scheme with different number of points, respectively. The mean value stays the

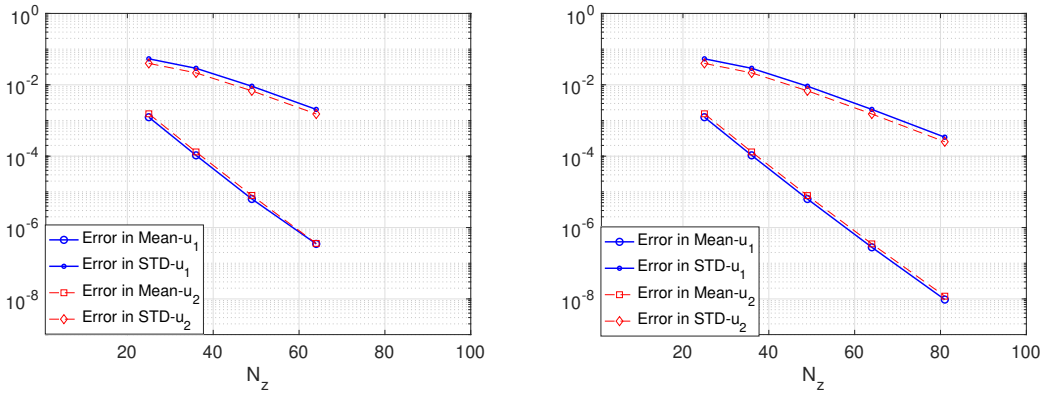

Figure 4.7: Shallow water equation (4.7). Case I. Errors in the mean and STD with respect to the number of collocation points N_z. DG scheme with $k = 2$ (left) and $k = 3$ (right). $N_x = 160$.

same for different number of points used in the SC method and the standard deviation has the similar feature when the number of points is large enough. Figures 4.11 and 4.12 show the mean and standard deviation of the numerical solution of Case II obtained by the SC scheme with different number of points, respectively. Both the mean and the standard deviation vary according to the number of points in the SC method. Moreover, the results of SC methods with 4×4 points agree well with those obtained by the stochastic Galerkin approach with basis polynomials being a tensor product structure based on the univariate polynomials of degree 3 in [36]. In contrast to Example 4.1, the mean of both random cases differs significantly from the deterministic solution using the mean values of the random parameters.

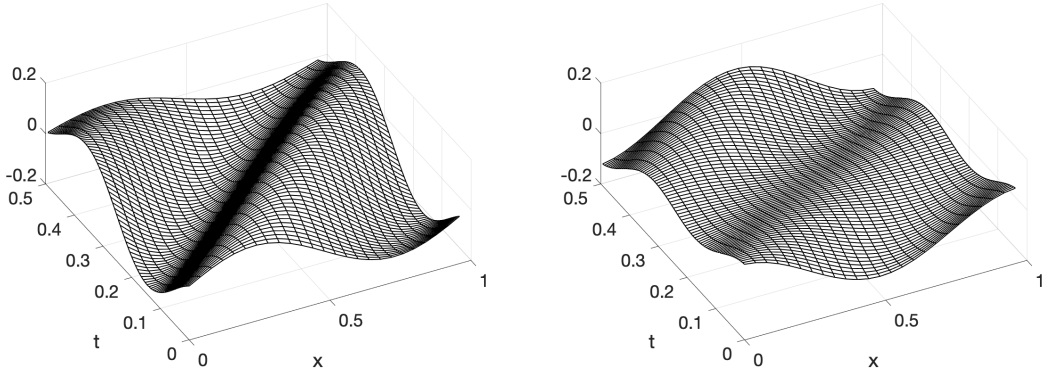

Figure 4.8: Shallow water equation. Deterministic solutions u_1 (left) and u_2 (right) using mean of the random parameters. $k = 2$.

Example 4.3. In this example, we consider the well-known Sod problem [41] which is a classical Riemann problem of the Euler equation (3.28) with the following initial conditions:

$$(\rho, u, p) = \begin{cases} (1,\ 0,\ 1), & x < \epsilon \\ (0.125,\ 0,\ 0.1), & x \geq \epsilon. \end{cases} \tag{4.9}$$

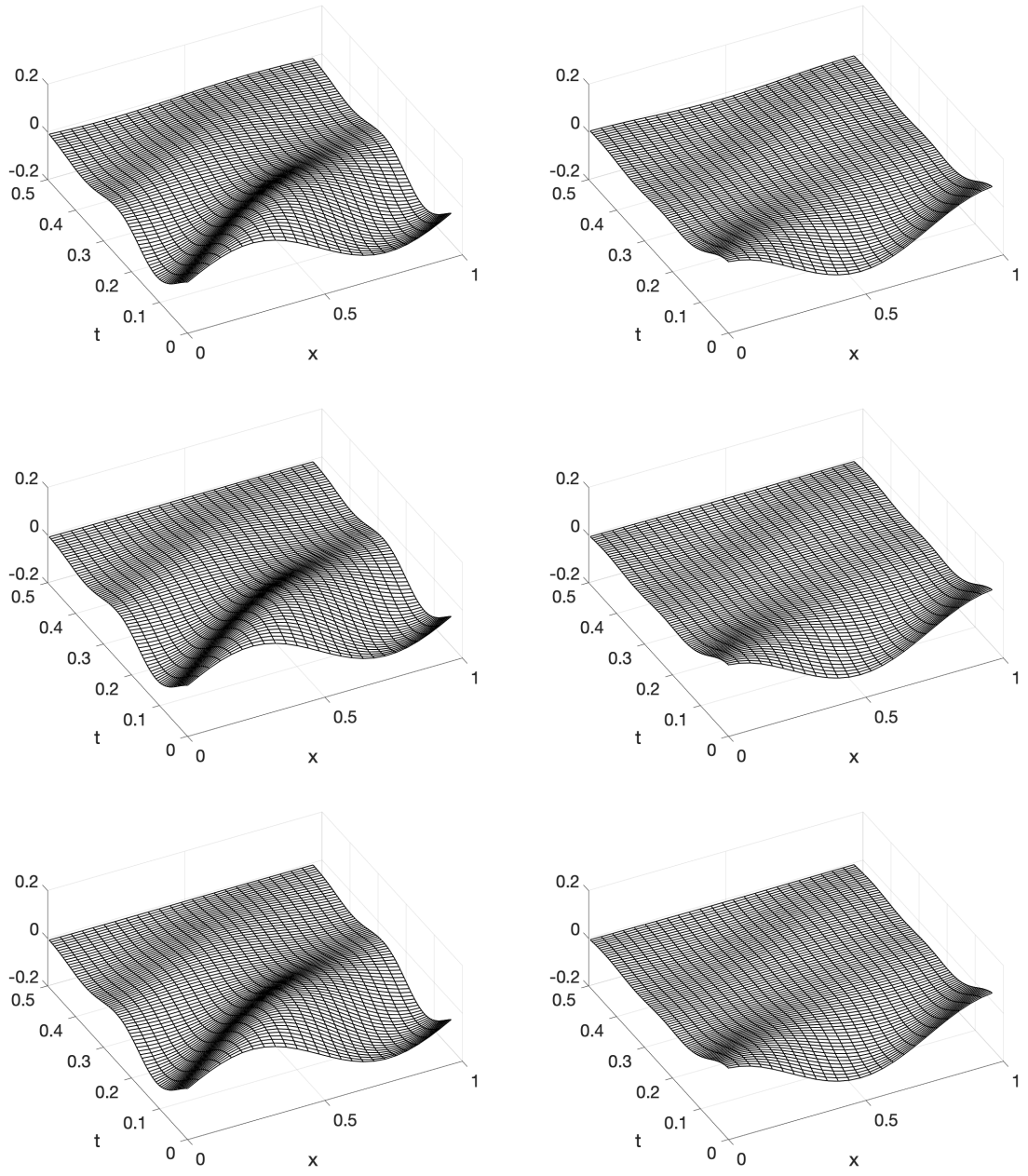

Figure 4.9: Shallow water equation. Case I. Mean of u_1 (left) and u_2 (right) obtained by the SC method with 4×4 (top), 10×10 (middle) and 16×16 (bottom) points. $k = 2$.

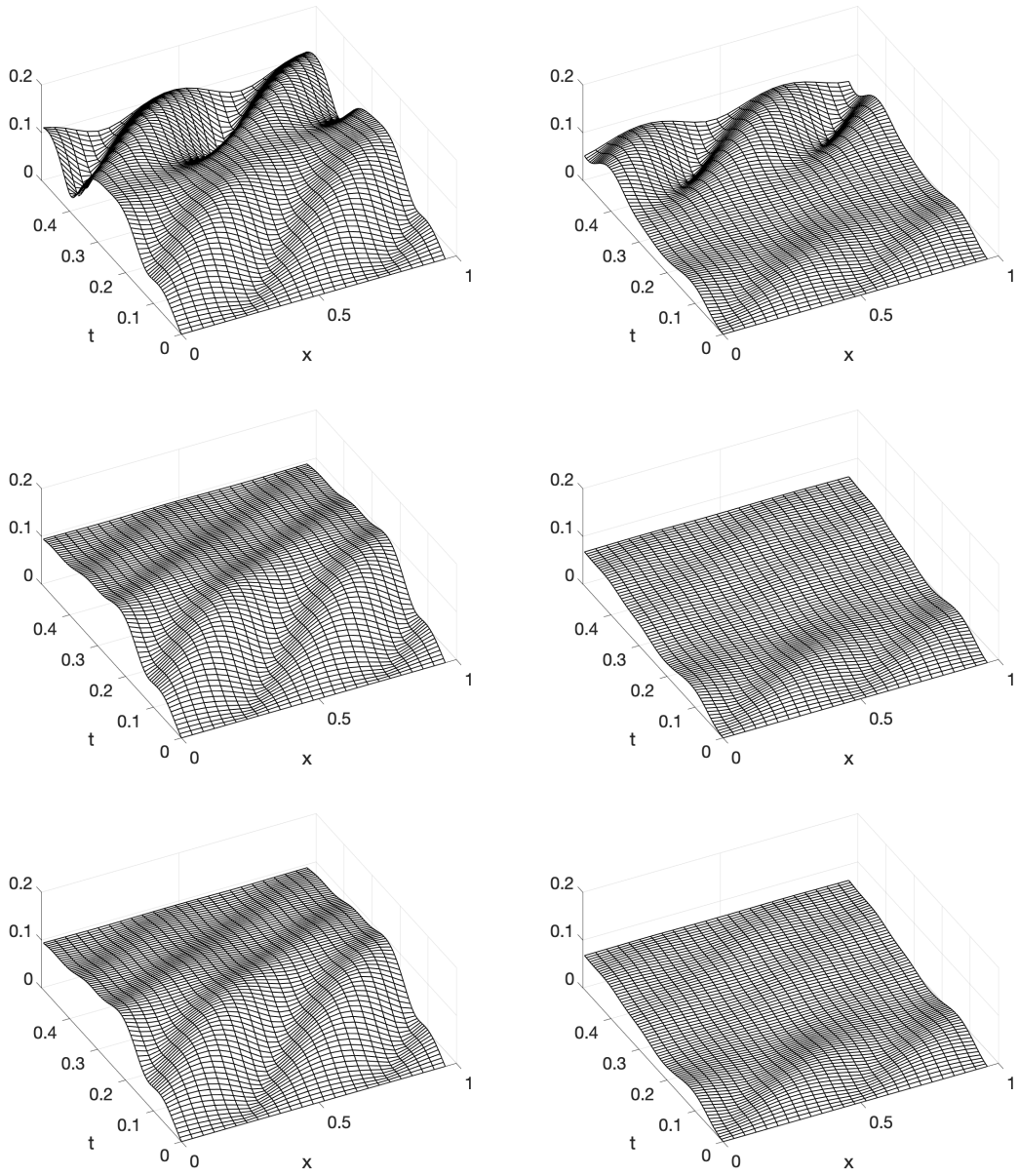

Figure 4.10: Shallow water equation. Case I. Standard deviation of u_1 (left) and u_2 (right) obtained by the SC method with 4×4 (top), 10×10 (middle) and 16×16 (bottom) points. $k = 2$.

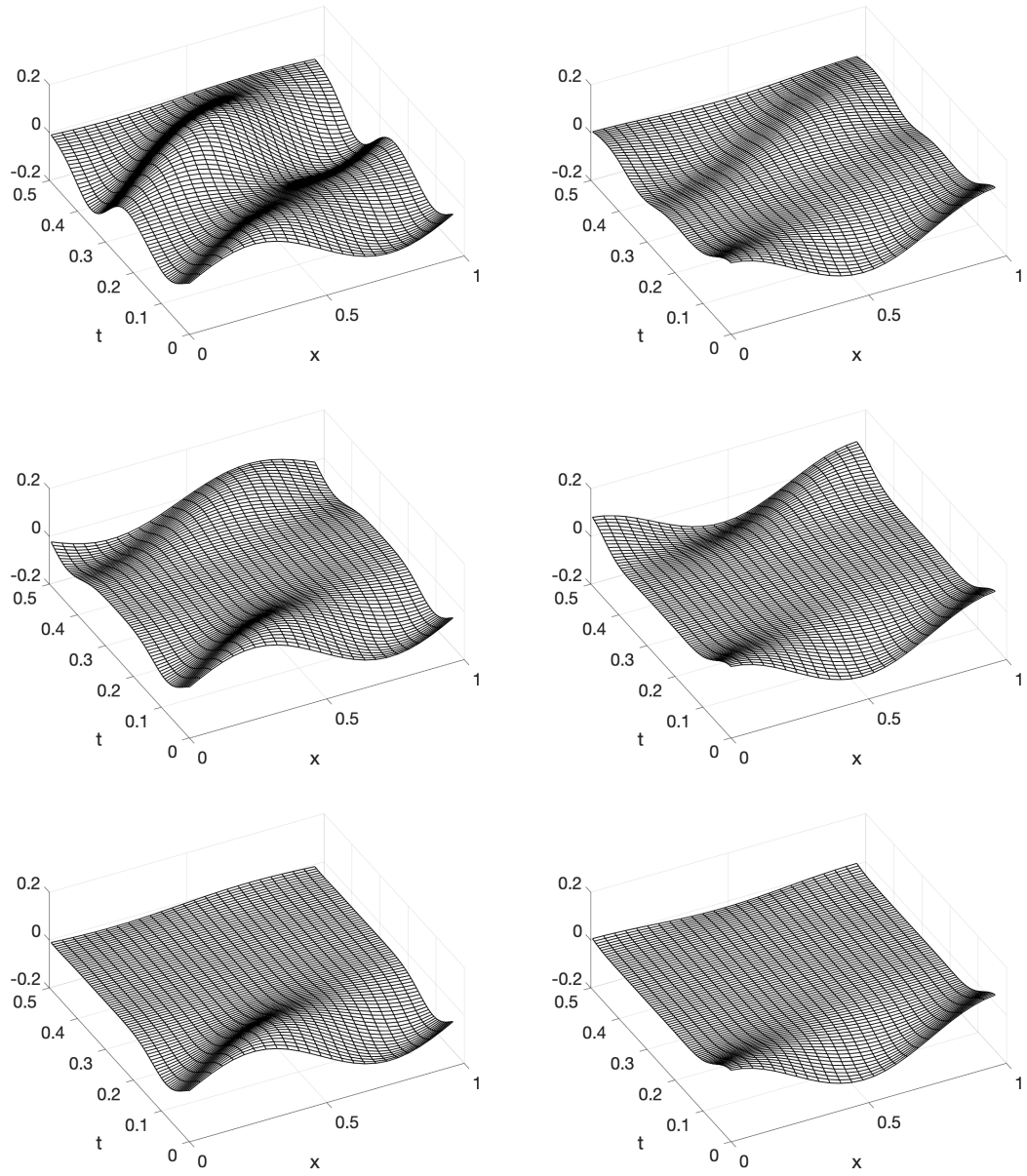

Figure 4.11: Shallow water equation. Case II. Mean of u_1 (left) and u_2 (right) obtained by the SC method with 4×4 (top), 10×10 (middle) and 16×16 (bottom) points. $k = 2$.

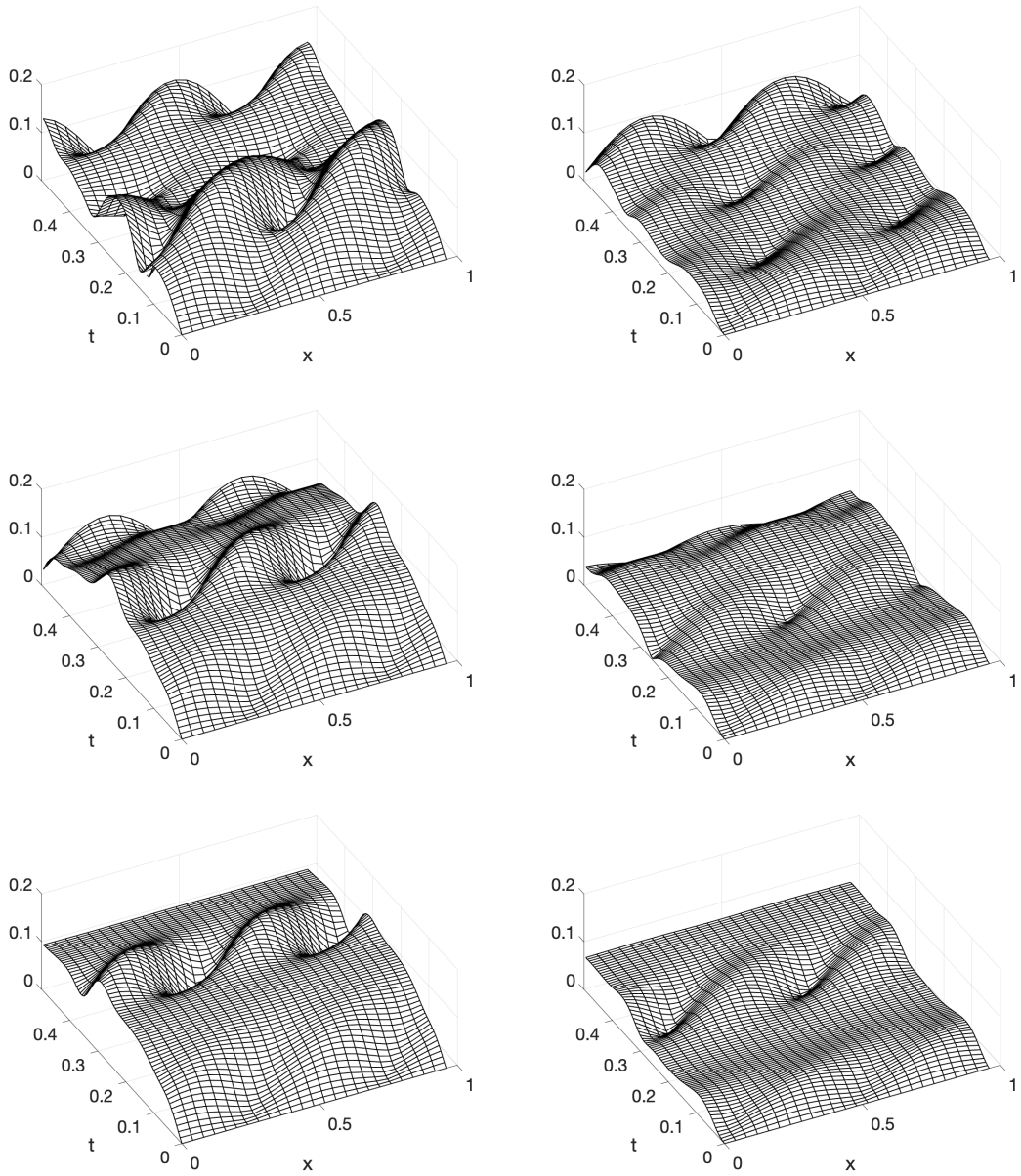

Figure 4.12: Shallow water equation. Case II. Stand deviation of u_1 (left) and u_2 (right) obtained by the SC with 4×4 (top), 10×10 (middle) and 16×16 (bottom) points. $k = 2$.

The computational domain is set as $[-0.5, 0.5]$. We investigate the impact of uncertainty on the Sod problem arising from either the ratio of specific heats γ in (3.28) or the initial shock position ϵ, i.e. the following two one-dimensional random cases:

- **Case I:** $\epsilon = 0$ and $\gamma = 1.5+0.1z$ with z being a uniformly distributed random variable on $[-1, 1]$ ($\gamma = 5/3$ for monatomic gas and $\gamma = 1.4$ corresponds to diatomic molecules).
- **Case II:** $\gamma = 1.4$ and $\epsilon = 0.05z$ with z being a uniformly distributed random variable on $[-1, 1]$.

The gPC basis for both cases is taken as the Legendre polynomial chaos, and thus Legendre-Gauss quadrature points are used in the collocation scheme. 20 Legendre-Gauss quadrature points are used to evaluate the mean and standard deviation of the exact solution. We perform numerical simulations by solving the resulted collocation scheme with the entropy stable DG method of $k = 2$ and $N_x = 130$. The Godunov flux is adopted at cell interfaces. Both entropy conservative fluxes (3.30) and (3.32) obtain equally good results. Therefore we only show the numerical results obtained by the flux (3.30) for Case I and by the flux (3.32) for Case II to save space.

The exact solution contains a left rarefaction wave, a middle contact discontinuity and a right shock wave. The standard DG scheme needs to apply limiters such as the positivity-preserving limiter to deal with the issues caused by negative density or negative pressure, which may be more complicated with the randomness in the system. Moreover the resulted deterministic system from the SG method for Euler equations is not hyperbolic [11]. However, after approaching the SG method in a pseudo-spectral fashion, we obtain a collocation scheme with suitable quadrature points $\{\zeta_m\}_{m=1}^{N_z}$, and then apply the entropy stable nodal DG scheme, which can be evolved without any limiter. For Case I, Figure 4.13 shows the mean and standard deviation of the numerical solution obtained with $N_z = 4$. We do not apply any limiter. We observe that the mean values of all waves are well resolved with slight over- and under-shoots at the right shock wave, and the values of standard deviation have peaked at the shock positions.

For Case II, the initial shock position is perturbed, which is more challenging. We first show the solutions at time $t = 0$ and $t = 0.13$ for three realizations of the random interface position. We do not apply any limiter and obtain good agreement between the numerical solutions and the exact solutions for each realization. For this challenging case, negative pressure or negative density may occur at some random shock positions. The positivity-preserving limiter [56] is applied to prevent negative density or negative pressure. We plot the mean and standard deviation of the numerical solution obtained with $N_z = 9$ in Figure 4.15, when the numerical solutions are better resolved with more collocation points in this case, while the numerical solutions of Case I stay almost the same with different sets of collocation points.

Example 4.4. In this example, we consider the Sod problem [41] with the following initial conditions:

$$(\rho, u, p) = \begin{cases} (1 + 0.1z_1,\ 0.05 + 0.05z_2,\ 1 + 0.1z_3), & x < 0 \\ (0.125 + 0.01z_4,\ 0,\ 0.1 + 0.01z_5), & x \geq 0. \end{cases} \tag{4.10}$$

where $\mathbf{z} = (z_1, z_2, z_3, z_4, z_5)$ are five independent, uniformly distributed random variables on $[-1, 1]$. The computational domain is set as $[-0.5, 0.5]$. $\gamma = 1.4$.

We perform numerical simulations using the entropy stable DG method with $k = 2$ and $N_x = 130$ for the spatial discretization. The Godunov flux is adopted at cell interfaces. Entropy conservative fluxes are taken as (3.32). For the stochastic discretization, we use the collocation scheme with Smolyak-type sparse grids constructed by Clenshaw-Curtis abscissas. Figure 4.16 shows the mean and standard deviation of the numerical solution obtained by Smolyak sparse grids of level 2. The mean and standard deviation of the exact solution are evaluated by the sparse grid quadrature rule of level 9. We do not apply any limiter. We observe

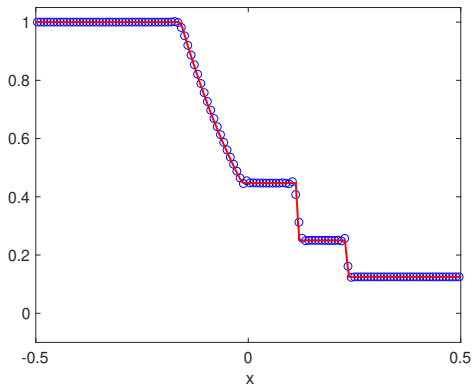

(a) mean of density

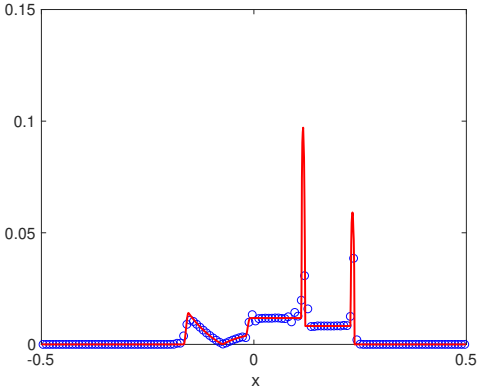

(b) STD of density

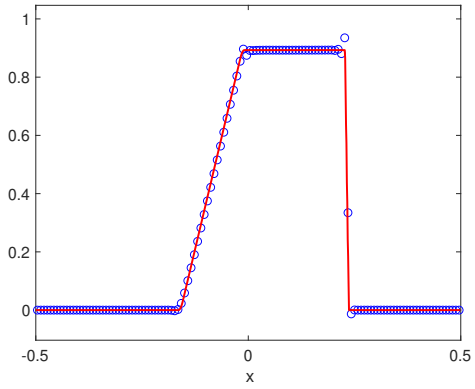

(c) mean of velocity

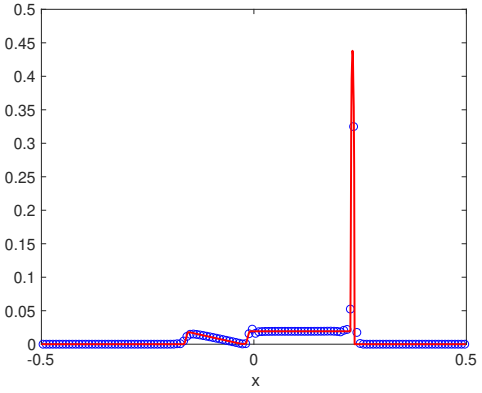

(d) STD of velocity

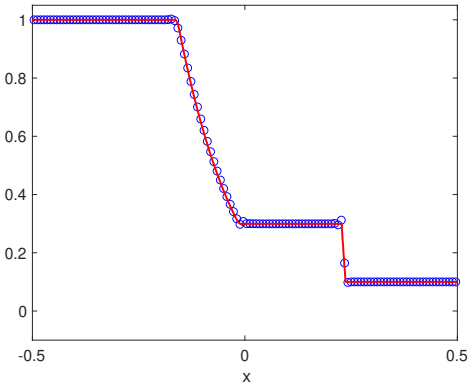

(e) mean of pressure

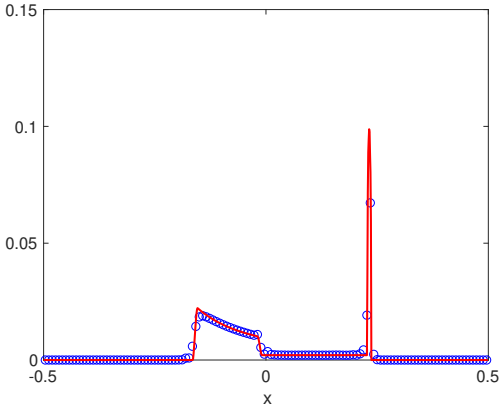

(f) STD of pressure

Figure 4.13: Sod's problem in Example 4.3. Case I. Solid line: exact solution; circle: numerical solution. Mean (left) and standard deviation (right) of density (top), velocity (middle) and pressure (bottom) at $t = 0.13$ (right). $N_z = 4$. $k = 2$. $N_x = 130$. We do not apply any limiter.

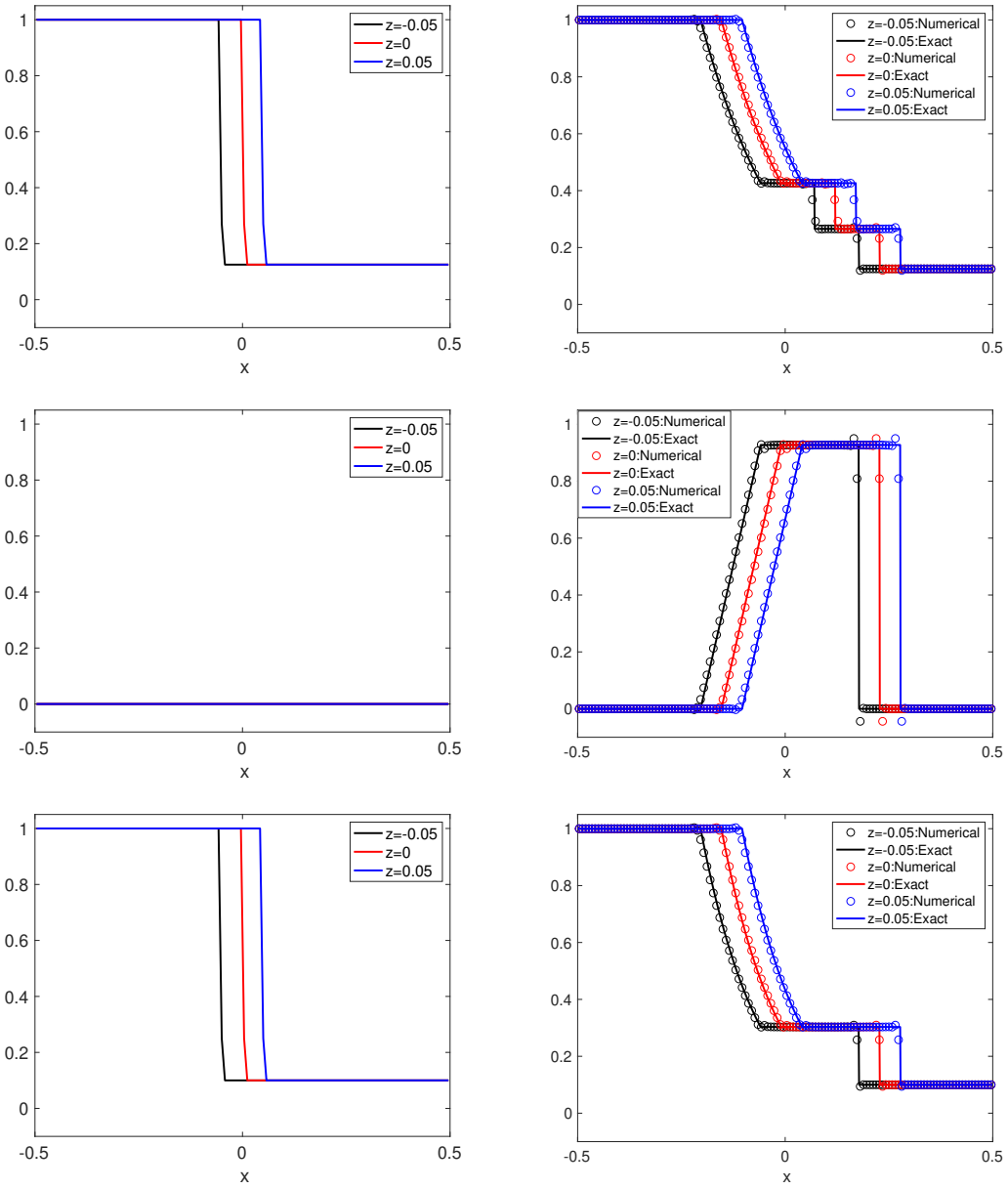

Figure 4.14: Sod's problem in Example 4.3. Case II. Density (top), velocity (middle) and pressure (bottom) at time $t = 0$ (left) and $t = 0.13$ (right) for three realizations of the random interface position. We do not apply any limiter.

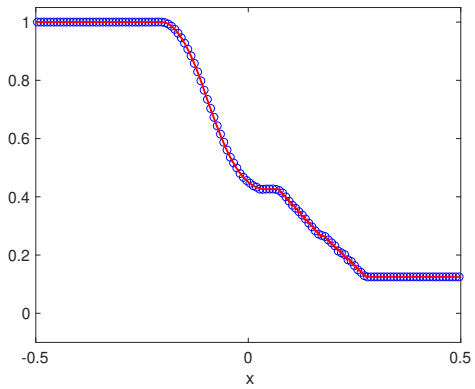

(a) mean of density

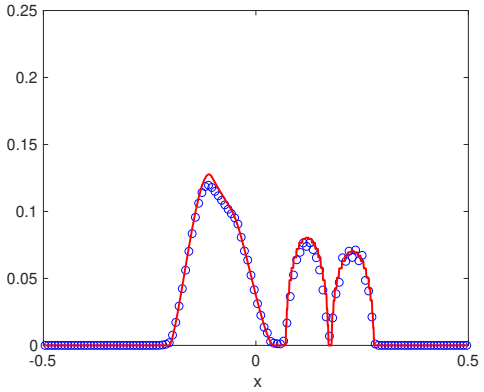

(b) STD of density

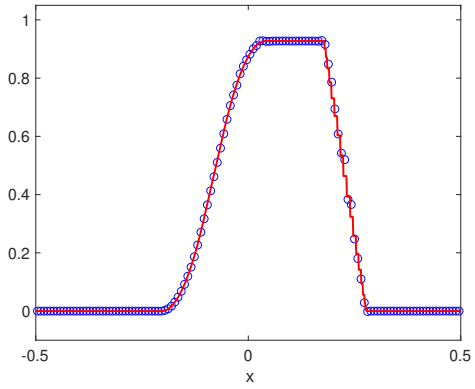

(c) mean of velocity

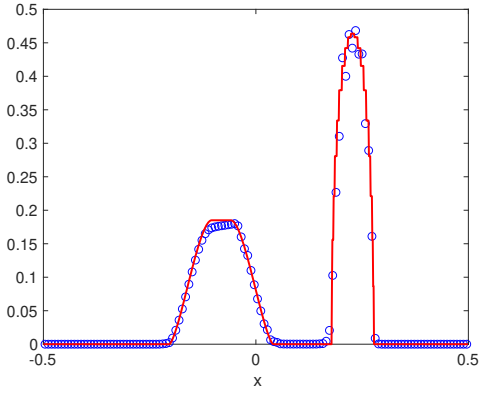

(d) STD of velocity

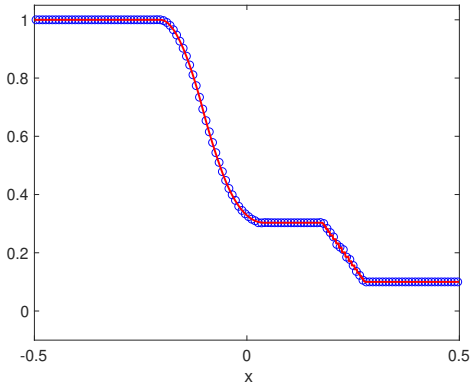

(e) mean of pressure

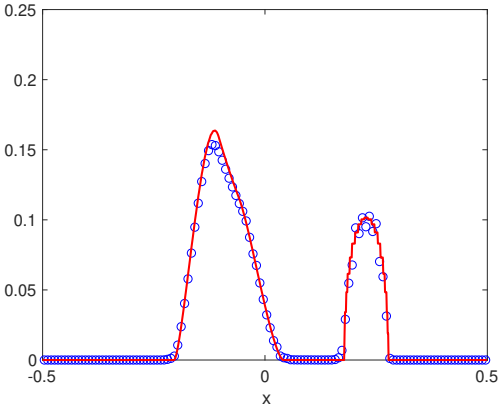

(f) STD of pressure

Figure 4.15: Sod's problem in Example 4.3. Case II. Solid line: exact solution; circle: numerical solution. Mean (left) and standard deviation (right) of density (top), velocity (middle) and pressure (bottom) at $t = 0.13$ (right). $N_z = 9$. $k = 2$. $N_x = 130$.

that the mean values of the rarefaction wave, contact discontinuity and the shock wave are all well resolved, and the values of the standard deviation have peaked at the shock positions.

5 Conclusion

In this paper, we investigate the impact of uncertainty on the hyperbolic systems. We discretize the uncertain hyperbolic system in the random space by the SG method, under a pseudo-spectral fashion, resulting a collocation type scheme on a set of suitable quadrature points. Then we apply the entropy stable DG method to discretize the spatial variable, coupling with the SSPRK method for time discretization, yielding an entropy stable solver for each node of the resulted collocation scheme. We demonstrate the accuracy and effectiveness of our numerical scheme by several hyperbolic systems with one-dimensional, two-dimensional and high-dimensional random variables. We remark here that although our focus in this paper is restricted to spatially one-dimensional hyperbolic systems, the idea can be extended to spatially multi-dimensional cases. For multi-dimensional hyperbolic systems, the SG method applied in the randoms space under a pseudo-spectral fashion can similarly lead to a collocation type scheme and the resulted scheme can be further approximated by suitable spatial discretizations and temporal discretizations.

Acknowledgments

X. Zhong was partially supported by the National Natural Science Foundation of China (NSFC) (Grant No. 11871428). C.-W. Shu was partially supported by NSF grant DMS-2010107 and AFOSR grant FA9550-20-1-0055. The authors would like to thank Dr. Tianheng Chen for many helpful discussions in the computation.

References

[1] I. Babuska, F. Nobile, and R. Tempone. A stochastic collocation method for elliptic partial differential equations with random input data. *SIAM Journal on Numerical Analysis*, 45(3):1005–1034, 2007.

[2] P. Chandrashekar. Kinetic energy preserving and entropy stable finite volume schemes for compressible Euler and Navier-Stokes equations. *Communications in Computational Physics*, 14(5):1252–1286, 2013.

[3] Q.-Y. Chen, D. Gottlieb, and J. S. Hesthaven. Uncertainty analysis for the steady-state flows in a dual throat nozzle. *Journal of Computational Physics*, 204(1):378–398, 2005.

[4] T. Chen and C.-W. Shu. Entropy stable high order discontinuous Galerkin methods with suitable quadrature rules for hyperbolic conservation laws. *Journal of Computational Physics*, 345:427–461, 2017.

[5] A. Chertock, S. Jin, and A. Kurganov. An operator splitting based stochastic Galerkin method for the one-dimensional compressible Euler equations with uncertainty. *preprint*, 2015. Available at https://chertock.wordpress.ncsu.edu/publications/.

[6] A. Chertock, S. Jin, and A. Kurganov. A well-balanced operator splitting based stochastic Galerkin method for the one-dimensional Saint-Venant system with uncertainty. *preprint*, 2015. Available at https://chertock.wordpress.ncsu.edu/publications/.

[7] B. Cockburn and C.-W. Shu. The Runge–Kutta discontinuous Galerkin method for conservation laws V: multidimensional systems. *Journal of Computational Physics*, 141(2):199–224, 1998.

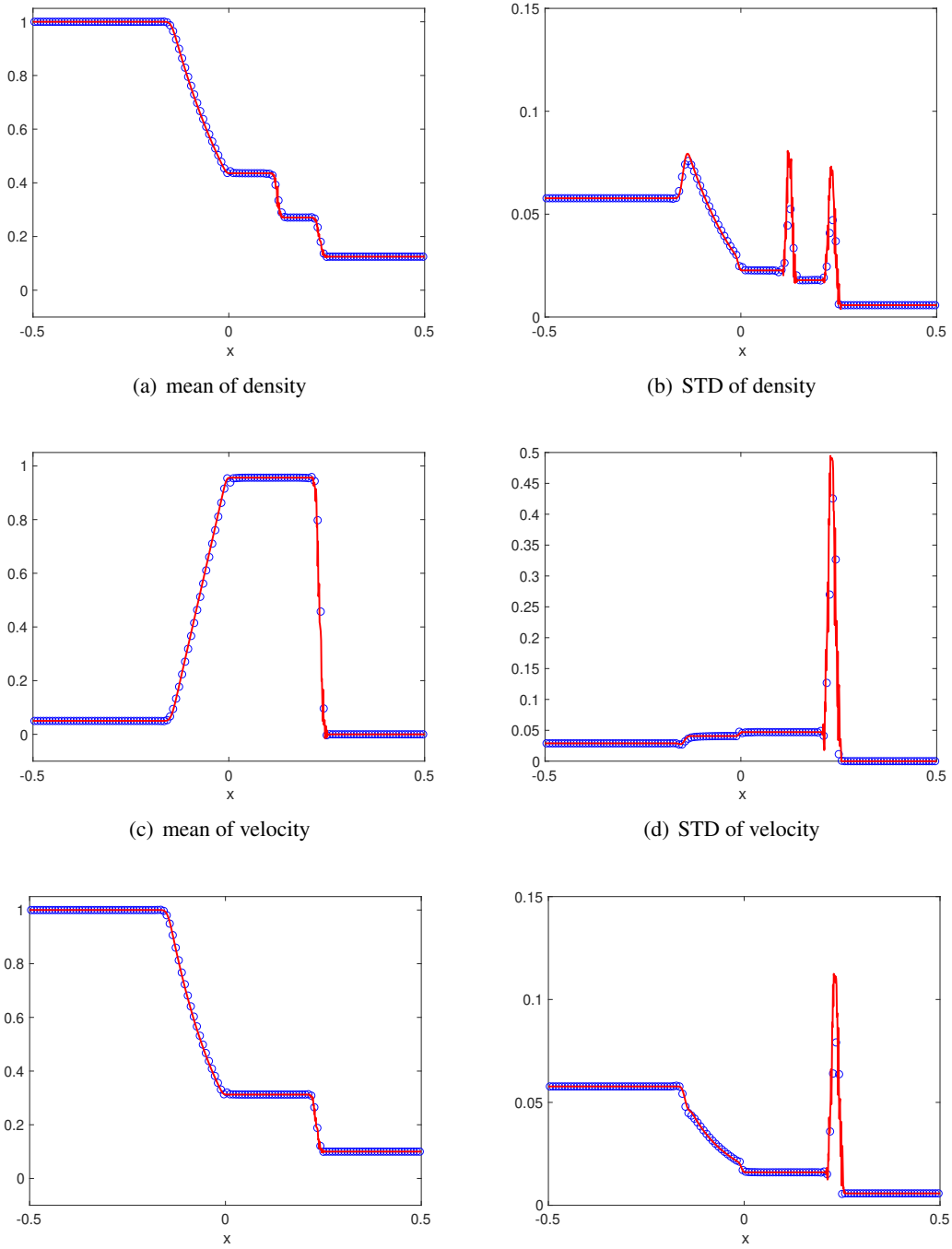

(a) mean of density

(b) STD of density

(c) mean of velocity

(d) STD of velocity

(e) mean of pressure

(f) STD of pressure

Figure 4.16: Sod's problem in Example 4.4. Solid line: exact solution; circle: numerical solution. Mean (left) and standard deviation (right) of density (top), velocity (middle) and pressure (bottom) at $t = 0.13$ (right). $k = 2$. $N_x = 130$. We do not apply any limiter.

[8] B. Cockburn and C.-W. Shu. Runge–Kutta discontinuous Galerkin methods for convection-dominated problems. *Journal of Scientific Computing*, 16(3):173–261, 2001.

[9] D. Dai, Y. Epshteyn, and A. Narayan. Hyperbolicity-preserving and well-balanced stochastic Galerkin method for shallow water equations. *SIAM Journal on Scientific Computing*, 43(2):A929–A952, 2021.

[10] D. Dai, Y. Epshteyn, and A. Narayan. Hyperbolicity-preserving and well-balanced stochastic Galerkin method for two-dimensional shallow water equations. *Journal of Computational Physics*, 452:110901, 2022.

[11] B. Després, G. Poëtte, and D. Lucor. Robust uncertainty propagation in systems of conservation laws with the entropy closure method. In H. Bijl, D. Lucor, S. Mishra, and C. Schwab, editors, *Uncertainty Quantification in Computational Fluid Dynamics*, Lecture Notes in Computational Science and Engineering, pages 105–149. Springer International Publishing, Cham, 2013.

[12] J. Dürrwächter, T. Kuhn, F. Meyer, L. Schlachter, and F. Schneider. A hyperbolicity-preserving discontinuous stochastic Galerkin scheme for uncertain hyperbolic systems of equations. *Journal of Computational and Applied Mathematics*, 370:112602, 2020.

[13] D. Funaro. *Polynomial Approximation of Differential Equations*. Number 8 in Lecture Notes in Physics. Springer-Verlag, Berlin Heidelberg, 1992.

[14] Z. Gao and T. Zhou. On the Choice of Design Points for least square polynomial approximations with application to uncertainty quantification. *Communications in Computational Physics*, 16(2):365–381, 2014.

[15] S. Gerster and M. Herty. Entropies and symmetrization of hyperbolic stochastic Galerkin formulations. *Communications in Computational Physics*, 27(3):639–671, 2020.

[16] S. Gerster, M. Herty, and A. Sikstel. Hyperbolic stochastic Galerkin formulation for the p-system. *Journal of Computational Physics*, 395:186–204, Oct. 2019.

[17] R. G. Ghanem and P. D. Spanos. *Stochastic Finite Elements: A Spectral Approach*. Springer New York, New York, NY, 1991.

[18] J. Giesselmann, F. Meyer, and C. Rohde. A posteriori error analysis and adaptive non-intrusive numerical schemes for systems of random conservation laws. *BIT Numerical Mathematics*, 60(3):619–649, Sept. 2020.

[19] E. Godlewski and P.-A. Raviart. *Numerical approximation of hyperbolic systems of conservation laws*. Number 118 in Applied mathematical sciences. Springer Nature, New York, NY, second edition edition, 2021.

[20] S. K. Godunov. An interesting class of quasilinear systems. *Dokl. Acad. Nauk SSSR*, 139:521–523, 1961.

[21] D. Gottlieb and S. A. Orszag. *Numerical Analysis of Spectral Methods: Theory and Applications*. Number CB26 in CBMS-NSF Regional Conference Series in Applied Mathematics. Society for Industrial and Applied Mathematics, Philadelphia, 1977.

[22] D. Gottlieb and D. Xiu. Galerkin method for wave equations with uncertain coefficients. *Commun. Comput. Phys*, 3(2):505–518, 2008.

[23] L. Guo, A. Narayan, T. Zhou, and Y. Chen. Stochastic collocation methods via ℓ_1 minimization using randomized quadratures. *SIAM Journal on Scientific Computing*, 39(1):A333–A359, 2017.

[24] B. Gustafsson, H. Kreiss, and J. Oliger. *Time dependent problems and difference methods*. Pure and Applied Mathematics. John Wiley & Sons, Inc, Hoboken, New Jersey, 2013.

[25] J. S. Hesthaven, S. Gottlieb, and D. Gottlieb. *Spectral Methods for Time-Dependent Problems*. Cambridge Monographs on Applied and Computational Mathematics. Cambridge University Press, Cambridge, 2007.

[26] F. Ismail and P. L. Roe. Affordable, entropy-consistent Euler flux functions II: Entropy production at shocks. *Journal of Computational Physics*, 228(15):5410–5436, 2009.

[27] S. Jin and R. Shu. A study of hyperbolicity of kinetic stochastic Galerkin system for the isentropic Euler equations with uncertainty. *Chinese Annals of Mathematics, Series B*, 40(5):765–780, 2019.

[28] S. Jin, D. Xiu, and X. Zhu. A well-balanced stochastic Galerkin method for scalar hyperbolic balance laws with random inputs. *Journal of Scientific Computing*, 67:1198–1218, 2016.

[29] O. P. Le Maı?tre, M. T. Reagan, H. N. Najm, R. G. Ghanem, and O. M. Knio. A stochastic projection method for fluid flow: II. Random process. *Journal of Computational Physics*, 181(1):9–44, 2002.

[30] R. J. LeVeque. *Numerical Methods for Conservation Laws*. Birkhäuser Verlag, Basel, 1990.

[31] L. Mathelin and M. Y. Hussaini. A stochastic collocation algorithm for uncertainty analysis. Technical Report NASA/CR-2003-212153, NASA Langley Research Center, Langley, Virginia, 2003.

[32] M. Mock. Systems of conservation laws of mixed type. *Journal of Differential Equations*, 37(1):70–88, 1980.

[33] F. Nobile, R. Tempone, and C. G. Webster. A sparse grid stochastic collocation method for partial differential equations with random input data. *SIAM Journal on Numerical Analysis*, 46(5):2309–2345, 2008.

[34] P. Pettersson, G. Iaccarino, and J. Nordström. A stochastic Galerkin method for the Euler equations with Roe variable transformation. *Journal of Computational Physics*, 257:481–500, 2014.

[35] G. Poëtte, B. Després, and D. Lucor. Uncertainty quantification for systems of conservation laws. *Journal of Computational Physics*, 228(7):2443–2467, 2009.

[36] R. Pulch and D. Xiu. Generalised polynomial chaos for a class of linear conservation laws. *Journal of Scientific Computing*, 51(2):293–312, 2011.

[37] L. Schlachter and F. Schneider. A hyperbolicity-preserving stochastic Galerkin approximation for uncertain hyperbolic systems of equations. *Journal of Computational Physics*, 375:80–98, 2018.

[38] F. Schneider and L. Schlachter. Hyperbolicity-preserving stochastic Galerkin method for hyperbolic systems with uncertainties. *PAMM*, 18(1):e201800160, 2018.

[39] C.-W. Shu and S. Osher. Efficient implementation of essentially non-oscillatory shock-capturing schemes. *Journal of Computational Physics*, 77(2):439–471, 1988.

[40] S. Smolyak. Quadrature and interpolation formulas for tensor products of certain classes of functions. *Soviet Math. Dokl.*, 4:240–243, 1963.

[41] G. Sod. A survey of several finite difference methods for systems of nonlinear hyperbolic conservation laws. *Journal of Computational Physics*, 27:1–31, 1978.

[42] E. Tadmor. The numerical viscosity of entropy stable schemes for systems of conservation laws. I. *Mathematics of Computation*, 49(179):91–103, 1987.

[43] E. Tadmor. Entropy stability theory for difference approximations of nonlinear conservation laws and related time-dependent problems. *Acta Numerica*, 12:451–512, 2003. Publisher: Cambridge University Press.

[44] T. Tang and T. Zhou. Convergence analysis for stochastic collocation methods to scalar hyperbolic equations with a random wave speed. *Communications in Computational Physics*, 8(1):226–248, 2010.

[45] M. A. Tatang, W. Pan, R. G. Prinn, and G. J. McRae. An efficient method for parametric uncertainty analysis of numerical geophysical models. *Journal of Geophysical Research: Atmospheres*, 102(D18):21925–21932, 1997.

[46] J. Tryoen, O. L. Maître, M. Ndjinga, and A. Ern. Intrusive Galerkin methods with upwinding for uncertain nonlinear hyperbolic systems. *Journal of Computational Physics*, 229(18):6485 – 6511, 2010.

[47] N. Wiener. The Homogeneous Chaos. *American Journal of Mathematics*, 60(4):897–936, 1938.

[48] K. Wu, H. Tang, and D. Xiu. A stochastic Galerkin method for first-order quasilinear hyperbolic systems with uncertainty. *Journal of Computational Physics*, 345:224–244, 2017.

[49] K. Wu, D. Xiu, and X. Zhong. A WENO-based stochastic Galerkin scheme for ideal MHD equations with random inputs. *Communications in Computational Physics*, 30(2):423–447, 2021.

[50] D. Xiu. Efficient collocational approach for parametric uncertainty analysis. *Communications in computational physics*, 2(2):293–309, 2007.

[51] D. Xiu. Fast numerical methods for stochastic computations: a review. *Commun. Comput. Phys.*, 5:242–272, 2009.

[52] D. Xiu. *Numerical Methods for Stochastic Computations: a Spectral Method Approach*. Princeton University Press, 2010.

[53] D. Xiu and J. S. Hesthaven. High-order collocation methods for differential equations with random inputs. *SIAM Journal on Scientific Computing*, 27(3):1118–1139, 2005.

[54] D. Xiu and G. Karniadakis. The Wiener–Askey polynomial chaos for stochastic differential equations. *SIAM Journal on Scientific Computing*, 24(2):619–644, 2002.

[55] Z. Xu and T. Zhou. On sparse interpolation and the design of deterministic interpolation points. *SIAM Journal on Scientific Computing*, 36(4):A1752–A1769, 2014.

[56] X. Zhang and C.-W. Shu. On maximum-principle-satisfying high order schemes for scalar conservation laws. *Journal of Computational Physics*, 229(9):3091–3120, 2010.

Statements and declarations

Funding: Author X. Zhong was partially supported by the National Natural Science Foundation of China (NSFC) (Grant No. 11871428). Author C.-W. Shu was partially supported by NSF grant DMS-2010107 and AFOSR grant FA9550-20-1-0055.

Financial interests: Both authors have no relevant financial or non-financial interests to disclose.

Data Availability Statement: Data sharing not applicable to this article as no datasets were generated or analysed during the current study.